OPEN ACCESS

Novenber 2021
ISSN 1684-5315
DOI: 10.5897/AJB
www.academicjournals.org

ACADEMIC JOURNALS
expand your knowledge

About AJB

The African Journal of Biotechnology (AJB) is a peer reviewed journal which commenced publication in 2002. AJB publishes articles from all areas of biotechnology including medical and pharmaceutical biotechnology, molecular diagnostics, applied biochemistry, industrial microbiology, molecular biology, bioinformatics, genomics and proteomics, transcriptomics and genome editing, food and agricultural technologies, and metabolic engineering. Manuscripts on economic and ethical issues relating to biotechnology research are also considered.

Indexing

CAB Abstracts, CABI's Global Health Database, Chemical Abstracts (CAS Source Index) Dimensions Database, Google Scholar, Matrix of Information for The Analysis of Journals (MIAR), Microsoft Academic, Research Gate

Open Access Policy

Open Access is a publication model that enables the dissemination of research articles to the global community without restriction through the internet. All articles published under open access can be accessed by anyone with internet connection.

The African Journals of Biotechnology is an Open Access journal. Abstracts and full texts of all articles published in this journal are freely accessible to everyone immediately after publication without any form of restriction.

Article License

All articles published by African Journal of Biotechnology are licensed under the Creative Commons Attribution 4.0 International License. This permits anyone to copy, redistribute, remix, transmit and adapt the work provided the original work and source is appropriately cited. Citation should include the article DOI. The article license is displayed on the abstract page the following statement:

This article is published under the terms of the Creative Commons Attribution License 4.0
Please refer to https://creativecommons.org/licenses/by/4.0/legalcode for details about Creative Commons Attribution License 4.0

Memberships and Standards

Academic Journals strongly supports the Open Access initiative. Abstracts and full texts of all articles published by Academic Journals are freely accessible to everyone immediately after publication.

All articles published by Academic Journals are licensed under the Creative Commons Attribution 4.0 International License (CC BY 4.0). This permits anyone to copy, redistribute, remix, transmit and adapt the work provided the original work and source is appropriately cited.

Crossref is an association of scholarly publishers that developed Digital Object Identification (DOI) system for the unique identification published materials. Academic Journals is a member of Crossref and uses the DOI system. All articles published by Academic Journals are issued DOI.

Similarity Check powered by iThenticate is an initiative started by CrossRef to help its members actively engage in efforts to prevent scholarly and professional plagiarism. Academic Journals is a member of Similarity Check.

CrossRef Cited-by Linking (formerly Forward Linking) is a service that allows you to discover how your publications are being cited and to incorporate that information into your online publication platform. Academic Journals is a member of CrossRef Cited-by.

Academic Journals is a member of the International Digital Publishing Forum (IDPF). The IDPF is the global trade and standards organization dedicated to the development and promotion of electronic publishing and content consumption.

Contact

Editorial Office: ajb@academicjournals.org

Help Desk: helpdesk@academicjournals.org

Website: http://www.academicjournals.org/journal/AJB

Submit manuscript online http://ms.academicjournals.org

Academic Journals
73023 Victoria Island, Lagos, Nigeria
ICEA Building, 17th Floor,
Kenyatta Avenue, Nairobi, Kenya.

Editor-in-Chief

Editorial Board Members

Table of Content

Vol. 20(11), pp. 431-439, November 2021
DOI: 10.5897/AJB2021.17409
Article Number: 7B9844668157
ISSN: 1684-5315

http://www.academicjournals.org/AJB

ACADEMIC JOURNALS
expand your knowledge

African Journal of Biotechnology

Full Length Research Paper

Genetic diversity analysis of sorghum [*Sorghum bicolor* (L.) Moench] races in Ethiopia using simple sequence repeats (SSR) markers

Gamachu Olani[1]*, Tileye Feyissa[2] and Tesfaye Disasa[3]

[1]Melkassa Agricultural Research Center, EIAR, Ethiopia.
[2]Holleta Agricultural Research Center, EIAR, Ethiopia.
[3]Institute of Biotechnology, Addis Ababa University, Ethiopia

Received 17 September, 2021; Accepted 2 November, 2021

Sorghum [*Sorghum bicolor* (L.) Moench], is believed to be originated in Ethiopia and Sudan. Although, many morphological and molecular diversity studies reveal the existence of genetic variations with sorghum populations, their distribution within basic races were not considered. Hence, the present study aimed to analyze the extent and distribution of genetic variation within basic Ethiopian sorghum landraces using SSR markers. A total of 107 landraces obtained from Ethiopian Biodiversity Institute (EBI) representing 12 ecological zones grouped according to their race types based on inflorescence and spiklet on field at their maturity time. Twelve SSR markers revealed a total of 110 alleles with average polymorphic content of 0.76 and the allele frequencies show 42 of them were rare (less than 0.05), 22 ranged from 0.05 to 0.1, while 46 of them were higher than 0.1. Expected and observed heterozygosity were 0.78 and 0.2, respectively. The genetic differentiation between populations were also moderate (FST=0.07 for races and 0.13 for E/zones) indicating continuous exchange of genes among them. Partitioning the total genetic variation also indicated 61.38 and 55.17% of the variations were among individuals within racial and zonal populations, respectively. Neighbor-Joining cluster analysis also indicated four major grouping of the landraces according to their racial groups where majority of race caudatum and durra form separate groups while intermediate durra-bicolor form two separate sub-clusters. Overall locus, the intra-racial population diversity showed the greatest genetic diversity (He=0.77 and 0.75) among race dura-bicolor and caudatum, respectively. Information with sorghum races along their important agronomic traits could be used for conservation and future breeding programs of sorghum.

Key words: *Sorghum bicolor*, races, genetic diversity, SSR.

INTRODUCTION

Sorghum [*Sorghum bicolor* (L.) Moench], a cultivated diploid (2n = 20) tropical cereal C4 grass plant, is the fifth most important cereal crop grown in the world. It is a monocotyledon plant of tropical origin, belonging to Poaceae family. Having nutritional composition similar to maize, starch is the major component of sorghum

*Corresponding author. E-mail: gamachuolani@gmail.com or tileye_feyissa@yahoo.com.

followed by protein, fat, and fiber (Council, 1996). The crop displays relatively high-water use efficiency compared to other cereals such as maize and wheat. Its wide adaptation to harsh environments, tolerance to stress conditions, diverse germplasm collections and its small genome size (710 Mb) made sorghum as an important botanical model crop for many tropical grasseswith complex genomes, which employ C4 photosynthesis. Sorghum is also the first crop genome of African origin to be sequenced (Dogget, 1965; Council, 1996).

Ethiopia is the second largest sorghum producer in Africa, after the Sudan and first among countries that have contributed many germplasm collections to the world collections of sorghum at both International Crop Research Institute for Semi-Arid Tropics (ICRISAT) and Griffin by National Plant Germplasm System (NPGS) (Demeke, 2013). It is one of the most important staple cereal crops after tef [*Eragrostis tef* (Zucc.) Trotter.] and maize (*Zea mays* L.) and holds third largest share of total cereal production with tef, maize, sorghum and wheat (*Triticum aestivum* L.) accounting for about 24.0, 16.8, 14.6, and 13%, respectively. Being an indigenous crop to Ethiopia, it is cultivated in almost all regions by subsistence farmers for various uses including as food and feed, house and fence construction, and prepare local beverages (CSA, 2014).

Though it was difficult to determine when and where sorghum domestication occurred, different studies suggested Ethiopia as a center of origin of sorghum due to the wide variation of the crop (McGuire, 2008; Vavilov, 1951). These also enable Ethiopian sorghum landraces as a source for an important agronomic trait including resistance to pest, sorghum midge (*Contarinia sorghicola*), and high lysine and protein contents (Fetene et al., 2011; Council, 1996). Sorghum had five basic races; namely bicolor, caudatum, durra, guinea and kafir. The entire races were differentiated morphologically based on their inflorescence, grain and glumes (Harlan and Wet, 1972). Clarissa et al. (2013) also described the geographic pattern of distribution of each race appears following the topography and climate variation present in Ethiopia. All the basic sorghum races except kafir also reported in Ethiopia. Accordingly, sorghum race durra is the main crop of the eastern highland region and mid elevation terrace of the north, while caudatum race is grown primarily in hot, dry valleys and lowland savannas in the south and west of Ethiopia. The intermediate race durra-bicolor predominates in the southwestern highland region, where cooler temperature and rain are higher than eastern and northern region. In contrast, bicolor and guinea races represent a very small part of Ethiopian sorghum diversity and both are mostly found in the Rift Valley region (House, 1985).

The diversity studies involving Ethiopian germplasms indicated the presence of huge genetic and morphological variations within their regions of origin and adaptation zones. Gebrekidan (1981) classified sorghum adaptation zones as: lowland (<1600 m above sea level (masl)), intermediate (1600-1900 masl) and highland (>1900 masl) in Ethiopia (Gebrekidan, 1981). Qualitative and quantitative studies, in addition to RAPD, AFLP and SSR markers utilized by different scholars also revealed the same amounts of variations among their collections (Ayana and Bekele, 1998; Geleta et al., 2006; Cuevas and Prom, 2013). SSR marker studies from Eritrean, Eastern Kenya, Benin and Zambia collections also showed presence of wide genetic diversity of sorghum bicolor in Africa mainly in Eastern regions (Tesfamichael et al., 2014; Catherine et al., 2016; Antoine et al., 2015; Ng'uni et al., 2011). The existence of imbalanced sorghum races in the sample collections of the different studies from Ethiopia might contribute to the overall observed genetic variation (Cuevas and Prom, 2013). Ethiopian Biodiversity Institute (EBI) collected large numbers of farmers' landraces though they do not have a racial category. Antoine et al. (2015) also recommended research on genetic diversity to integrate both botanical races and morpho-physiological characteristics of the crops for better preservation of sorghum genetic resources. In addition, morphological studies involving germplasms from Ethiopia and Eritrea show the greatest share of variation observed were carried by their panicle compactness and shape, which is 31% (Ayana and Bekele, 1998). Therefore, racially partitioned diversity studies among founding major basic races and representative of the whole collections of Ethiopian adaptation zones were lacking. Hence, the present study aimed at analyzing the genetic variation within basic Ethiopian sorghum races.

MATERIALS AND METHODS

Germplasm collections

The accessions used for this study were landrace accessions collected by EBI. A total of 107 sorghum landrace accessions were selected based on phonological evaluation of inflorescence and spiklet types at their maturity time in order to define the racial classifications in 2015/2016 cropping season at Arsi Negelle Research Station based on their passport data. The materials were received and planted along with other germplasm by Melkassa Sorghum Improvement Program. In addition to the difference in head morphology, geographical distribution of the sorghum races across the country were considered for selection of their adaptation zones. All basic sorghum races except kafir and from the intermediate types, widely distributed durra-bicolor were included. The selected 107 sorghum landrace collections were grouped based on their source of origins into 12 populations, which each contained 9 landrace accessions for DNA extraction and genotyping study.

DNA extraction and PCR amplification

The seeds of collected sorghum genotypes were planted at National Agricultural Biotechnology Research Center (NABRC), Holetta, on seedling tray in greenhouse for germination. Genomic

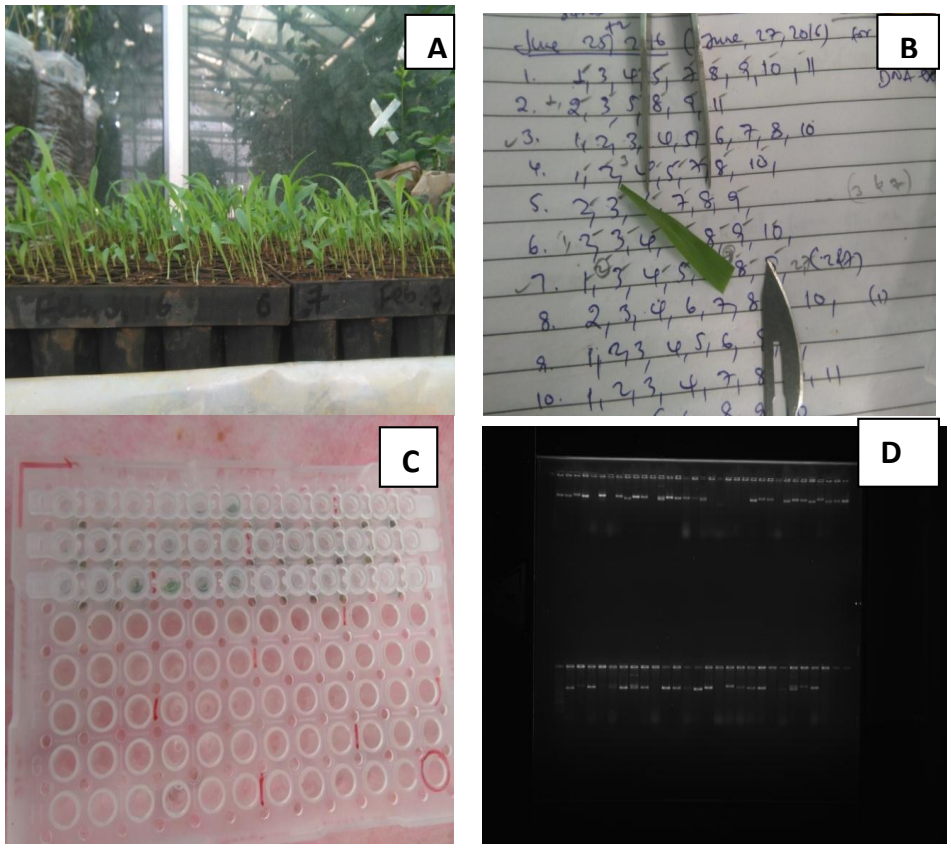

Figure 1. A: Procedures for the throughput (commonly called Dirty method) DNA extraction protocols (Sorghum seeds planted for their germination to be used for DNA extraction after two weeks, B: About 50 mm^2 single leaf per accession were used, C: the leaves were transferred to PCR plates sequentially and 50 µl Buffer A added to each before their incubation at 95ºC in thermocycler for 10 minutes and the same amount of Buffer B added, and briefly mixed to be used for PCR amplification, and D: Confirmation of PCR amplification using marker xtxp258).

DNA was extracted from 2-week old seedlings using fresh leaves according to Xin et al. (2003) utilizing only two ordinary buffers that made the genomic DNA available for PCR amplification reactions. Approximately 50 mm^2 single leaf sample per landraces was harvested to PCR plates for their DNA extraction. The two buffers include: Buffer A made from 100 mM NaOH and 2% Tween 20, which are made fresh from their stock solutions (10M NaOH and 20% Tween 20) and Buffer B consisting of 100 mM Tris-HCl and 2 mM EDTA, whose pH set to 2.0. Once the buffers are ready, the genomic DNA was extracted with the following procedures: (1) Approximately 30 mm^2 leaf tissue transferred to 96-well plates; (2) 50 µL buffer A added and incubated for 10 min at 95°C in thermo cycler; (3) 50 µL buffer B was added and mixed at moderate speed; (4) Aliquot PCR mixture to 96-well plates at a reaction volume of 20 µL/well; (5) and finally transfer approximately 1.5 µL DNA from the crude DNA plates to PCR plates with a 96-pin applicator (Figure 1). Twelve polymorphic SSR primer pairs (Table 1) were selected for genotyping the selected 107 sorghum landraces. PCR amplification was carried out in 20 µL reaction volume containing 1.5 µL crude genomic DNA, 2.25 µl PCR buffer with $MgCl_2$ (17.5 mM), 1.8 µl of dNTPs (10 mM), 0.45 µl each of forward and reverse primers (10 mM), 0.133 µl of Taq Polymerase (5U), 0.1% BSA (Bovine Serum Albumin) (w/v) and 1% PVP (w/v). The amplifications were carried out with thermo cycler programmed for initial denaturation at 94°C for 15 min, the second denaturation at 94°C for 30 s, annealing at 50°C for 1 min, extension at 72°C for 2-min, final elongation at 72°C for 20 min and holding temperature at 4°C until conclusion. PCR products were analyzed by loading the 3 µl PCR products along with a 3 µL loading dye mixed with Gel Red (at a ratio of 1000:1) using 3.5% agarose gel electrophoresis run with 100 V for 3 h along with DNA Ladder (500 bp bioline Hyperladder V).

Data collection and statistical analysis

Once gel images were taken with Gel documentation, the PCR fragments were scored manually by estimating their base pair size as compared with known fragments size ladders that were run gel electrophoresis along with each accession. The number of alleles (N), major allele frequency (A), observed heterozygosity (Ho), expected heterozygosity/gene diversity (He) and polymorphism information content (PIC) for each SSR locus were analyzed using PowerMarker 3.25 (Liu and Muse, 2005).

Pairwise genetic distance was calculated as given by Nei and Takezaki (1994). Further, the allelic data were subjected to estimate the genetic distances using simple matching coefficients and the

Table 1. Lists of 13 Selected Sorghum SSR Markers used with their primer sequences.

No.	SSR marker name	Forward primer sequence	Reverse primer sequence	Repeat motif	Expected allele size
1	*Xtxp211*	TCAACGGCCAATGATTTCTAAC	AGGTTGCGAATAAAAGGTAATGTG	(CT)23	206
2	*Xtxp258*	CACCAAGTGTCGCGAACTGAA	GCTTAGTGTGAGCGCTGACCAG	(AAC)19	222
3	*Xgap001*	TCCTGTTTGACAAGCGCTTATA	AAACATCATACGAGCTCATCAATG	(AG)16	240
4	*Xtxp295*	AAATCATGCATCCATGTTCGTCTTC	CTCCCGCTACAAGAGTACATTCATAGCTTA	(TC)19	175
5	*Xtxp008*	ATATGGAAGGAAGAAGCCGG	AACACAACATGCACGCATG	(TG)31	148
6	*Xtxp012*	AGATCTGGCGGCAACG	AGTCACCCATCGATCATC	(CT)22	193
7	*Xtxp312*	CAGGAAAATACGATCCGTGCCAAGT	GTGAACTATTCGGAAGAAGTTTGGAGGAAA	(CAA)26	154
8	*Xtxp141*	TGTATGGCCTAGCTTATCT	CAACAAGCCAACCTAAA	(GA)23	152
9	*Xtxp285*	ATTTGATTCTTCTTGCTTTGCCTTGT	TTGTCATTTCCCCCTTCTTTCTTTT	(CTT)11 CTC(CTT)1	231
10	*Xtxp021*	GAGCTGCCATAGATTTGGTCG	ACCTCGTCCCACCTTTGTTG	(AG)18	172
11	*Xtxp357*	CGCAGAAATACGATTG	GCTATCTGGAGTAACTGTGT	(GT)10	273
12	*SbKAKG1*	AGCATCTTACAACAACCAAT	CTAGTGCACTGAGTGATGAC	(ACA)9	142

genotypes were clustered using Neighbor Joining method. Both the clustering analysis and PCoA were done using DARwin software ver. 6.0.13. The data were tested for presence of population structure and analysis of molecular variance (AMOVA) was performed to separate the total molecular variance into components between groups, within groups and intra population variation using Arlequin version 3.0 software (Excoffier et al., 2005). Pairwise genetic differentiation between different groups was assessed with fixation index (Weir and Clark, 1984) as implemented in Arlequin software.

RESULTS AND DISCUSSION

Marker polymorphism

A total of 110 alleles were separated using 12 SSR markers (Table 2). The number of alleles per marker ranged from 5 (*xtxp298* and *xtxp258*) to 18 (*xtxp211*) with an average of 9.2 alleles per locus. *Xtxp298* and *xtxp012* hold the lowest and highest number of genotypes (6 and 19, respectively) with an average of 15.8 genotypes per locus. The allele frequencies varied from 0.005 for marker *xtxp285* to 0.648 for *xtxp312* with an overall average frequency of 0.109. The mean number of alleles per locus observed in this study was higher than similar SSR studies with accessions from North Eastern Benin, 7 (Antoine et al., 2015), Zambia, 4.4 (Ng'uni et al., 2011), Eastern Kenya, 5.05 (Catherine et al., 2016), Eritrea, 4.8 (Tesfamichael et al., 2014) and Egypt, 7.3 (El-Awady et al., 2008), and Ethiopian collections in combination with other countries (Agrama and Tuinstra, 2003). However, it is lower than Cuevas and Prom (2013) population structure and diversity study for 137 Ethiopian germplasm conserved at USDA-ARS National Plant Germplasm System, that is 14 per locus. Out of the total 110 alleles, specifically 42 alleles had frequencies below 0.05 (rare alleles), 22 alleles had a frequency within 0.05 to 0.10 (common alleles) while the rest 46 alleles had frequency higher than 0.10 becoming an abundant allele. While across all races average number of frequencies ranged from 7.17 in intermediate durra-bicolor to 4.75 in race bicolor whereas mean gene diversity ranged from 0.32 (bicolor) to 0.22 (durra). Their mean number of alleles within the different races ranged from 7.17 (durra-bicolor) to 4.75 (bicolor). Likewise, their gene diversity ranged from 0.77 for durra-bicolor to 0.70 for durra, guinea and bicolor (not shown).

Their polymorphic information content (PIC) varied from 0.51 (*xtxp312*) to 0.91 (*xtxp211*) with an average of 0.76 and the expected and observed heterozygosity (gene diversity and heterozygosity respectively) ranged from 0.54

Table 2. Basic statistics of 12 SSR markers using powermarker V3.25 software.

Marker	MAF	N_G	N_A	H_e	H_o	PIC
xtxp258	0.359	8.0	5.0	0.755	0.071	0.72
xtxp008	0.284	16.0	8.0	0.813	0.257	0.79
xtxp012	0.257	19.0	9.0	0.841	0.229	0.82
xtxp312	0.648	8.0	6.0	0.543	0.042	0.51
xtxp141	0.294	13.0	10.0	0.820	0.221	0.80
xtxp211	0.108	33.0	18.0	0.917	0.619	0.91
xtxp285	0.163	35.0	16.0	0.900	0.471	0.89
xtxp021	0.388	14.0	8.0	0.763	0.117	0.73
xtxp357	0.380	9.0	9.0	0.751	0.024	0.71
SbKAKG1	0.383	14.0	9.0	0.758	0.107	0.73
xgap001	0.282	15.0	7.0	0.812	0.234	0.79
xtxp298	0.338	6.0	5.0	0.738	0.014	0.69
Mean	**0.324**	**15.8**	**9.2**	**0.784**	**0.200**	**0.76**

MAF- Major allele frequency; N_G- number of genotypes; N_A - Total number of Alleles; H_e- GeneDiversity; H_o- Heterozygosity; PIC-polymorphic information content.

(*xtxp312*) to 0.92 (*xtxp211*) and 0.014 (*xtxp298*) to 0.62 (*xtxp211*), respectively.

Higher polymorphism within the present Ethiopian landraces observed may be indication of the extensive and regular seed exchange farming system within farmers of Ethiopia (Mcguire, 2000). This form of seed migrations also adds allelic variations to landraces avoiding genetic drift. Thus, the observed rare alleles could be useful as an additional source of important agronomic traits. In fact, Sorghum, a genus having evolved across a wide range of environments in Africa, exhibits a great range of phenotypic diversity and numerous resistances to abiotic and biotic stresses (Dogget, 1965). It is cultivated in all regions of Ethiopia from 400 to 2500 masl. Hence, the wider agro-ecological diversity of Ethiopian climates from where the samples were collected and the presence of wider morphological variations observed within them might contribute to its genetic variations (Mcguire, 2000).

Similar findings by Cuevas and Prom (2013), and to a certain extent Agrama and Tuinstra (2003) also reported average PIC values 0.78 and 0.622, respectively. However, the observed PIC value is higher than that of Geleta et al. (2006), Antoine et al. (2015) and Catherine et al. (2016) who reported 0.46, 0.33 and 0.49, respectively. This may be the result of low numbers of accessions considered in their studies and sample collections represented are from specific areas of agro-ecologies. Although sorghum is considered as self-pollinating species, cross-pollinations between sorghum landraces are believed to be as high as 7%, and can even reach 70% in certain races in particular environments. The observed high allelic frequencies could also arise from outcrossing within wild and weedy relatives (House, 1985; Dogget, 1965).

AMOVA analysis

Partitioning the total variation of 107 Ethiopian sorghum landraces using 12 SSR markers revealed the presence of 61.38 and 55.17% variations explained by individual differences within race and their ecological zones, respectively. In contrast, the variations among the two populations are very small (6.86% among races and 12.9% among zones). A considerable amount of its total variation was recorded across the overall individual landraces that is 31.7% with a moderate degree of gene differentiation among racial populations in terms of allele frequencies, FST: 0.073 (Table 3). The moderate genetic differentiation among the present populations in terms of allele frequency also indicated the continuous exchange of genes between them. This finding also supports earlier studies by Cuevas and Prom (2013) who found genetic differentiation of 0.10 among 137 Ethiopian sorghum maintained at NPGS. However, Ganapathy et al. (2012) reported high estimate of fixation index (FST=0.35, P=0.001) using 82 Indian genotypes.

Cluster analysis and pairwise genetic dissimilarity

Neighbor-joining analysis indicated four major clusters (Figures 2 and 3). The first cluster, representing the largest numbers of accessions of all races in scattered manner, formed two sub-clusters inside; one with mainly of caudatum and another uniformly intermixed race. The second cluster most uniquely contained mainly durra race (18/27, 67% of the total population representing the race) along with rare numbers of caudatum and durra-bicolor (3 and 4). Exceptionally, no bicolor race clustered under this group, while only a single guinea represented. Like the

Table 3. Analysis of Molecular Variance (AMOVA) using 12 SSR markers by Alrequin ver 3.5.1.3.

Components	Source of variation	d.f.	Sum of squares	Variance component	Percentage variation
Sorghum Races	Among populations	4	31.93	0.22	6.86
	Among individuals within populations	102	500.81	1.95	61.38
	Within individuals	107	108.00	1.01	31.76
	Total	213	664.76	3.18	-
Ecological Zones	Among populations	11	129.49	0.41	12.90
	Among individuals within populations	95	427.26	1.74	55.17
	Within individuals	107	108.00	1.01	31.93
	Total	213	664.76	3.16	-

*Average F-statistics across all loci becomes: *Population_race*, FIS: 0.66, FST: 0.07 and FIT: 0.68, and *population_E/Zones*, FIS: 0.63, FST: 0.13 and FIT: 0.68, *p*-value=0.0001.

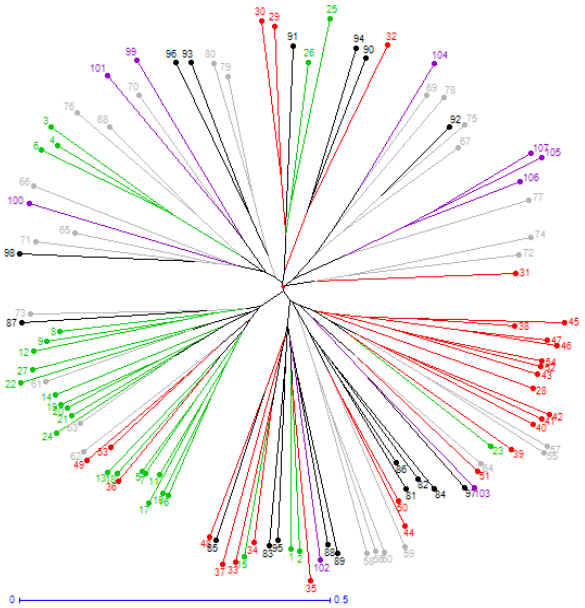

Figure 2. Cluster analysis of 107 Ethiopian sorghum landraces (Green: race durra, accession 1-27; Red: caudatum, accession 28-54; Gray: durra-bicolor, accessions 55-80; Black: race guinea, accession 81-98; and Purple: race bicolor, accessions from S/N 99 to 107.

first cluster, the third cluster also formed two sub-clusters and most intermediate durra-bicolor structured in one sub-cluster along with other race types. Under the final cluster 4, majority of race durra-bicolor contained along with a single caudatum and guinea race, and rare number (that is 4) of bicolor. RFLP analysis on 94 accessions also reported the greatest amount of diversity within races bicolor and guinea when racially classified. They also reported the race bicolor appeared highly variable and did not form a specific group. Hence, it was believed to be distributed wherever sorghum is grown (Wang et al., 2013). The most unique and clustered race in PCoA, race durra, is abundant in Ethiopian and Sudan as well and Harlan and Wet (1972) also reported settlers in warm highlands of Ethiopia have used the durra sorghum as their foundation of their agricultural system almost 500 years ago. These may be the reason why durra-bicolor intermediate race were also abundant in the country. In addition, caudatum, a race being adapted to harsh conditions, are found most commonly in areas

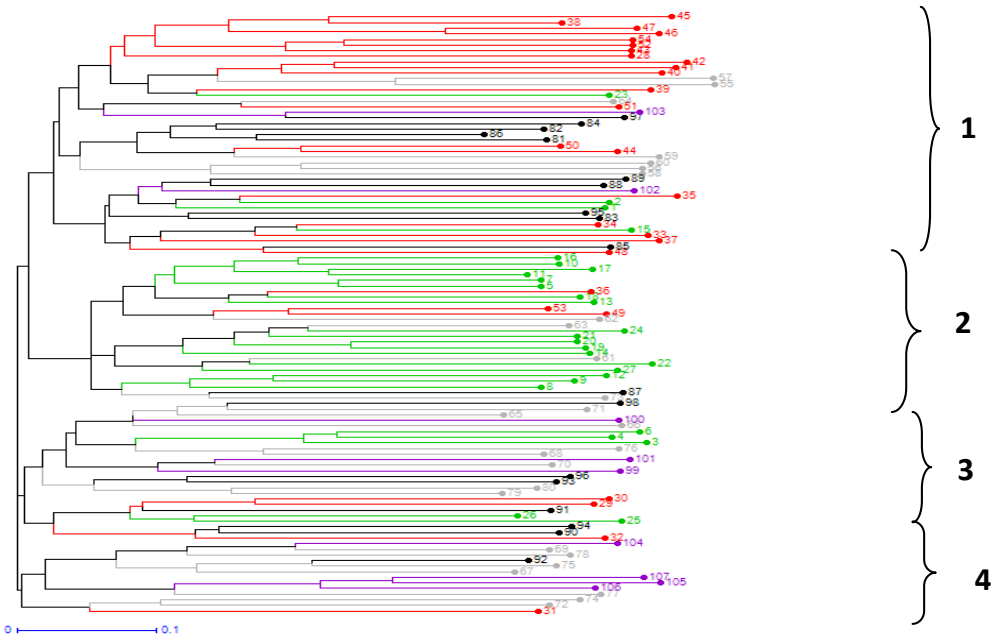

Figure 3. Dendogram for 107 Ethiopian landraces based on unweighted neighbor joining (Green: race durra, accession 1-27; Red: caudatum, accession 28-54; Gray: durra-bicolor, accessions 55-80; Black: race guinea, accession 81-98; and Purple: race bicolor, accessions from S/N 99 to 107).

receiving 250 to 1,300 mm of rain annually (Stemler et al., 1977). The bicolor and guinea, representing the smallest parts of Ethiopian diversity, distributed evenly across all clusters except the bicolor race which did not form a group within durra race cluster.

Matrix of pairwise genetic distance of the racial population relationships (Table 5) indicated the existence of the highest dissimilarity between race bicolor and durra (highest genetic distance, 0.19) while the lowest score was registered between intermediate durra-bicolor and guinea (0.06). Whereas, among populations of different ecological zones pairwise genetic distance ranged from 0.0096 to 0.286 between West Wollega and Illubabor, and between Central and South Tigray and East Harerge, respectively. The least genetic distance between West Wollega and Illubabor (0.0096) may be due to the close proximity of the two zones where free seed exchange might occur. In contrast, the greatest dissimilarity (0.286) recorded were between central and south Tigray and east Harerghe zones (Table 4).

CONCLUSION AND RECOMMENDATIONS

In general, the racial classification among *S. bicolor* could be used for *in-situ* and *ex-situ* conservation and genetic dissimilarity with their respective agronomic characteristics favors the future crops germplasm breeding programs. In this regard, Ethiopian sorghum races were structured into four major clusters according to their racial difference except for race bicolor and guinea. Bicolor found being scattered within other groups. The greatest genetic distance found between bicolor and caudatum while between the Ethiopian zones, central and south Tigray and east Harerghe. There was also a huge variation observed among the populations of both racial classification and ecological zones (61.38 and 55.17%, respectively). The greater mean number of alleles per locus (9.2) and PIC value of 0.76 in the present study also indicate the presence of high genetic diversity among Ethiopian sorghum collections and the discriminatory power of the selected markers. There is also a moderate levels of genetic differentiation among races (FST= 0.07) and Ethiopian sorghum producing zones (FST=0.13). Hence, racial groups could also be used as representation of the germplasm collection along with the commonly known diverse agro-ecological and zonal collections and their adaptation zones.

In line with the present study, the future research areas should include molecular studies along with the morphological components using markers linked to specific agronomic traits to enable the use of racial groupings within sorghums in its breeding areas. In addition, classification of the national sorghum germplasm collections according to their race was also needed since the Ethiopian landraces have been used as

Table 4. Population pairwise FSTs_according to E/Zones.

Correlation	1	2	3	4	5	6	7	8	9	10	11	12
1	0.000											
2	0.162	0.000										
3	0.169	0.255	0.000									
4	0.118	0.073	0.058	0.000								
5	0.230	0.258	0.180	0.140	0.000							
6	0.275	0.230	0.286	0.128	0.144	0.000						
7	0.244	0.243	0.136	0.109	0.156	0.222	0.000					
8	0.102	0.167	0.066	0.072	0.211	0.202	0.166	0.000				
9	0.124	0.221	0.157	0.126	0.254	0.230	0.200	0.010	0.000			
10	0.180	0.198	0.250	0.114	0.178	0.152	0.200	0.118	0.158	0.000		
11	0.136	0.123	0.096	0.099	0.203	0.212	0.168	0.081	0.099	0.136	0.000	
12	0.202	0.237	0.181	0.108	0.186	0.189	0.151	0.068	0.097	0.122	0.119	0.000

Average gene diversity over loci: 0.587146 ± 0.321973 and numbers in bold were the highest and lowest distance scored. 1:N/Wello, 2:S/Wello, 3:E/Harerge, 4:Metekel, 5:Gambella(Z1), 6:Cent_S/Tigray, 7:Jimma, 8:Illubabor, 9:W/Wellega, 10:N/Shewa, 11:Bench_Maji and 12:E/Shewa.

Table 5. Pairwise genetic dissimilarity among sorghum races (Distance method: Pairwise differences).

Correlation	Durra	Caudatum	Durra_bicolor	Guinea	Bicolor
Durra	-				
Caudatum	0.08609	-			
Durra_bicolor	0.05741	0.08787	-		
Guinea	0.07009	0.07734	**0.05728**	-	
Bicolor	**0.18937**	0.11858	0.07156	0.09562	-

The bolded numbers show the highest and lowest genetic distance scored between races.

the source of important traits.

CONFLICT OF INTERESTS

The authors have not declared any conflict of interests.

ABBREVIATIONS

dNTPs, Deoxynucleotide triphosphates; **EBI,** Ethiopian Biodiversity Institute; **NPGS,** National Plant Germplasm System; **PIC,** polymorphic information content; **PVP,** polyvinylpyrrolidone; **RAPD,** random amplified polymorphic DNA; **RFLP,** restriction fragment length polymorphism; **SSR,** simple sequence repeats.

ACKNOWLEDGEMENTS

The authors thank the technical staff at National Agricultural Biotechnology Research Center, Holetta for generously helping technically throughout the time in their laboratory and Melkassa management staff's in easing the work with financial issues

REFERENCES

Agrama HA, Tuinstra MR (2003). Phylogenetic diversity and relationships among sorghum accessions using SSRs and RAPDs. African Journal of Biotechnology 2(10):334-340.

Antoine AM, Hubert AS, Paulin S, Clement A, Corneille A, Rollande AD (2015). Genetic diversity of Sorghum bicolor (L.) Moench) landraces from Northwestern Benin as revealed by microsatellite markers. African Journal of Biotechnology 14(16):1342-1353.

Ayana A, Bekele E (1998). Geographical patterns of morphological variation in sorghum (Sorghum bicolor (L.) Moench) germplasm from Ethiopia and Eritrea: Qualitative characters. Hereditas 129(3):195-205.

Catherine WM, Reuben MM, Duncan TK, Steven MR, Arthur K (2016). Genetic variability of sorghum landraces from lower Eastern Kenya based on simple sequence repeats (SSRs) markers. African Journal of Biotechnology 15(8):264-271.

Clarissa TK, Jef AD, Stephen K (2013). The Genepool of Sorghum bicolor and its improvements. In A. H. Paterson (Ed.), Genomics of the Saccharinae, Plant Genetics and Genomics:Crops and Models (pp. 23-39). Texas, USA: Springer.

Council NR (1996). Lost crops of Africa. Volume 1, Grains. Washigton, DC: National Academy Press.
CSA (2014). Report on area and production of major crops: private peasant holdings of Meher season (Vol. 1). Addis Ababa, Ethiopia.
Cuevas HE, Prom LK (2013). Assessment of molecular diversity and population structure of the Ethiopian sorghum (*Sorghum bicolor* (L.) Moench) germplasm collection maintained by the USDA-ARS National Plant Germplasm using SSR markers. Genetic resources and Crop Evolution 60(6):1817-1830.
Demeke MDF (2013). Analysis of Incentives and Disincentives for Sorghum in Ethiopia. Rome: MAFAP, FAO.
Dogget H (1965). Disruptive section in crop development. Nature 4981:279-280.
El-Awady M, Youssef SS, Selim EEM, Ghonaim MM (2008). Genetic diversity among Sorghum bicolor genotypes using simple sequence repeats (SSRs) markers. Arab Journal of Biotechnology 11(2):181-192.
Excoffier L, Laval G, Schneider S (2005). Arlequin (version3.0): An integrated software package for population genetics data analysis. Switzerland: 3012 Berne.
Fetene M, Okori P, Gudu S, Mneney EE, Tesfaye K (2011). Delivering New Sorghum and Finger Millet Innovations for Food Security and Improving Livelihoods in Eastern Africa. Kenya, Nairobi: ILRI.
Ganapathy KN, Gomashe SS, Rakshit S, Ambekar SS, Ghorade RB, Biradar BD, Patil JV (2012). Genetic diversity revealed utility of SSR markers in classifying parental lines and elite genotypes of sorghum (*Sorghum bicolor* L. Moench). Australian Journal of Crop Science 6(11):1486-1493.
Gebrekidan B (1981). Salient features of the sorghum breeding strategies used in Ethiopia. Ethiopian Journal of Agricultural Sciences 3:97-104.
Geleta N, Labuschagne MT, Viljoen CD (2006). Genetic diversity analsis in sorghum germplasm as estimated by AFLP, SSR and morpho-agronomical markers. Biodiversity and Conservation 15(10):3251-3265.
Harlan JR, Wet JM (1972). Simplified classification of cultivated sorghum. Crop Science 12(2):172-176.
House LR (1985). A Guide to Sorghum Breeding (Second ed.). India: International Crops Research Institute for the Semi-Arid Tropics.
Liu K, Muse S (2005). PowerMarker: integrated analysis environment for genetic marker data. Bioinformatics 21:2128-2129.
Mcguire S (2000). Farmers' management of sorghum diversity in Eastern Ethiopia. In C Almekinders, W deBoef (Eds.), Encouraging Diversity: The Conservation and Development of Plant Genetic Resources (pp. 43-48). London: Intermediate Technology.
McGuire SJ (2008). Securing access to seed: Social relations and Sorghum seed exchange in Eastern Ethiopia. Human Ecology 36(2):217-229.
Nei M, Takezaki N (1994). Estimation of Genetic Distances and Phylogenetic Trees from DNA Analysis. In Proceedings of the 5th World Congress on Genetics applied to Livestock production, Vol.21 (pp. 405-412). Ontario, Canada: University of Guelph.
Ng'uni D, Geleta M, Bryngelsson T (2011). Genetic diversity in sorghum (Sorghum bicolor (L.) Moench) accessions of Zambia as revealed by simple sequence repeats (SSR). Hereditas 148(2):52-62.
Stemler A, Harlan J, de Wet J (1977). The sorghums of Ethiopia. Economic Botany 31:446-460.
Tesfamichael T, Githiri SM, Kasili RW, Skilton R, Solomon M, Nyende A (2014). Genetic diversity analysis of Eritrean sorghum (*Sorghum bicolor* (L.) Moench) germplasm using SSR markers. Molecular Plant Breeding 5(13):1-12.
Vavilov N (1951). The Origin, Variation, Immunity and Breeding of Cultivated Plants. USA: The Chronica Botanica Co.
Wang YH, Upadhyaya HD, Burrell AM, Sahraeian SM, Klein RR, Klein PE (2013). Genetic structure and linkage disequilibrium in a diverse representative collection of the C4 model plant, *Sorghum bicolor*. Genetics 3:783-793.
Weir BS, Clark C (1984). Estimating F-Statistics for the analysis of population structure. Evolution 38(6):1358-1370.
Xin Z, Velten J, Oliver M, Burke J (2003). High-throughput DNA extraction method suitable for PCR. Biotechniques 34(4):820-824.

Vol. 20(11), pp.440-450, November 2021
DOI: 10.5897/AJB2021.17348
Article Number: C5B5D9B68176
ISSN: 1684-5315

http://www.academicjournals.org/AJB

ACADEMIC JOURNALS
expand your knowledge

African Journal of Biotechnology

Review

Advances on the application of non-coding RNA in crop improvement

Diriba Guta Dekeba

Ethiopian Institute of Agriculture Research, National Agricultural Biotechnology Research Center, Holeta, Oromia, Ethiopia.

Received 14 April, 2021; Accepted 26 July, 2021

Thanks to committed plant breeding researchers over the few decades, many problems associated with food supply and qualities have been improved. Food security is an exceptionally serious worldwide issue via world climate change, the increase in human population, and the use of plants for bioethanol production in current years. Improved tolerance to abiotic and biotic stress, resistance to herbicides, improved yield, and plants with wonderful nutritional value are essential goals of crop improvement. RNAi applications are the modern innovation that can assist in the solution for these issues. A natural protection mechanism against invading viruses, nucleic acids, and transposons non-coding RNAs (ncRNAs), are identified as effector molecules in RNA-mediated gene silencing and used in the genetic modification of crops. These ncRNAs are concerned with the regulation of growth, development, and response to stress at the transcriptional and translational levels. Improving crop yields is the final purpose of molecular plant breeding. ncRNAs, along with transfer RNAs (tRNAs) and ribosomal RNAs (rRNAs), as well as small non-coding RNAs (sncRNAs) and the long non-coding RNAs (lncRNAs), have been recognized as essential regulators of gene expression in plants in plant immunity and adaptation to abiotic and abiotic stages biotic stress.

Key words: Crop improvement, long RNA, ncRNA, RNA interference, small RNA.

INTRODUCTION

The world population is growing rapidly; however, world food security is still threatened in recent years via climate change, the increase in human population and the use of plants for bioethanol production in recent years (FAO, 2020). In addition, the future capacity to meet the world's food security needs has come to be unstable as the area of arable and cultivated land continues to decrease. These issues and threats have led scientists to look for options to increase crop productivity. Proponents of new technologies, which include recombinant DNA, have a promise in current green transformation, with genetically engineered plants which include transgenes achieving focused traits (Wheeler and von Braun, 2013; Sang and Chanseok, 2016; Bader et al., 2020; Mezzetti et al., 2020).

E-mail: dirguta46@gmail.com Tel: +251921437346.

Non-coding RNAs refer to transcripts that no longer code for proteins; however play vital regulatory roles within the cell, which precludes the possibility of the production of exogenous protein products. Non-coding RNA can be a gene silencing phenomenon that involves sequence-specific gene legislation encapsulated via double-stranded RNA, resulting in inhibition of protein production (Zheng and Qu, 2015; Brant and Budak, 2018; Yan et al., 2020, 2021).

Some classes of regulatory ncRNAs especially regulate a single goal gene, while others modulate more than one gene at the genome-wide level via various molecular mechanisms. These cumulative consequences advise that regulatory ncRNAs may want to be possible goals for molecular plant breeding (Zhou and Luo, 2013).

Non-coding RNAs are divided into functionally vital RNAs such as transfer RNA (tRNA), ribosomal RNA (rRNA), small non-coding RNAs, including Micro-RNAs (miRNAs), small interfering RNAs (siRNAs), piwi-interacting RNAs (piRNAs), and the long non-coding RNAs (lncRNAs). Two lncRNAs that have been substantially studied are the X-inactivation-specific transcript (XIST) and the HOX-antisense-intergenic RNA (HOTAIR) (Renyi and Jiankang, 2014; Santosh et al., 2014; Brant and Budak, 2018).

Post-transcriptional gene silencing (PTGS) is mentioned in many organisms; fungi, animals, and plants (Zhou and Luo, 2013; Brant and Budak, 2018). These products are the result of non-coding dsRNA, the DICER or Dicer-like enzyme, which performs this cleavage. Small non-coding RNA consists of an RNA-induced silencing complex (RISC) and Argonaute proteins (AGOs). Drosha and Pasha are part of the microprocessor protein complex. Drosha and Dicer are RNase III enzymes, Pasha is a dsRNA-binding protein, while Argonauts are RNase H enzymes (Wilson and Doundna, 2013; Kamthan et al., 2015; Brant and Budak, 2018).

The goals of this review had been to discuss non-coding RNA and its use in plant improvement. The RNA interferences in the adaptation of plants to the environment serve the tolerance to abiotic stress and the plant protection towards biotic stress. The RNA interference increases the yield potential of plants, such as manipulating plant improvement and improving nutrition. They modulate a broad range of gene regulatory networks via regulating a specific subset of downstream genes that are closely associated to agricultural traits such as seed maturation, flower development, pathogen resistance, and other abiotic stress resistance.

Natures of non-coding RNAs (ncRNAs)

Ribosomal RNA (rRNA)

Ribosomal RNA is the most abundant small non-coding RNA molecule that is made up of 4-10% cellular RNA. They are translation machines in so far as they translate the genetic information into a corresponding polypeptide chain in a mRNA template-directed manner (Rodnina and Winter Meyer, 2011). The mRNA sequence starts with the begin codon of AUG and is followed by termination codon signaling for subsequent folding into its functional state (Crick, 1970). The ribosomes in eukaryotes are more complex than in prokaryotic ones; in general, ribosomes have three exclusive binding sites; A (aminoacyl) site, the P (peptidyl) site and the E (parent) site in the interface between the subunits. The mRNA that binds to the 30S subunit can regularly move one codon at a time during peptide elongation (Crick, 1970).

The ribosomal RNA is about 60% by weight rRNA and 40% by weight protein and additionally includes two most important rRNAs and 50 or more proteins. The 60S subunit incorporates (three rRNAs 5S, 5.8S, 28S and about forty proteins) and the 40S subunit contains (an18S rRNA and about 30 proteins). The LSU rRNA acts as a ribozyme and catalyzes the formation of peptide bonds (Anita et al., 2013).

Transfer RNA (tRNA)

Transfer RNA is the link between mRNA and the peptide sequence in transfer RNA (tRNA). There is an enzyme that can understand both tRNA and an anticodon, which is complementary to the mRNA codon associated to this amino acid, and couples it to a highly standardized free energy complex known as aminoacyl-tRNA at the rate of ATP hydrolysis (Sharp at el., 1985). The mRNA binds to the 40s ribosomal subunit, followed by using the binding of the initiator tRNA loaded with formylated methionine to the P site in a reaction step that is considerably accelerated by the three initiation factors. As soon as the mRNA and the initiator tRNA are successfully bound, the large 60S subunit binds to form an 80s initiation complex, releasing the eIF factors. With the mRNA in the correct reading frame, the initiator tRNA in the P-site and the empty A-site programmed with the first interior codon of the protein to be synthesized. The ribosome has now left the initiation phase and has entered the peptide elongation phase (Valle et al., 2003).

Short non-coding RNAs

Micro RNA (miRNA)

Micro-RNA is the party of the small non-coding RNA (20-22nt) with partially double-stranded stem loop structures, which regulates negative gene expression in both animals and plants. It is transcribed by the RNA polymerase II enzyme and, after transcription, cleaved by the Dicer-like 1

(DCL1) enzyme and transported into the cytoplasm and incorporated into the Argonaut (AGO) protein. Mature miRNA is produced in various processes and incorporated into the protein RISC (RNA-induced Stille complex). Mature single miRNA that incorporates the RISC protein binds with other complementary mRNA sequences to produce the protein (Khraiwesh et al., 2012).

Small interfering RNA (siRNA)

Small interfering RNAs are the parts of small non-coding RNA that have the function of facilitating post-transcriptional gene silencing (PTGS) by breaking down mRNA. Small interfering RNA is generated from RNA double strands that are nearly perfectly complementary and cleaved by DCL2, DCL3 and DCL4 to produce siRNA duplexes 22nt, 24nt and 21nt, respectively (Sang and Chanseok, 2016). The other cofactors of siRNA are the RNA-dependent RNA polymerases 2 and 6 (RDR2, RDR6), SUPPRESSOR OF GENE SILENCING 3 (SGS3) and the plant-specific DNA-dependent RNA polymerases IV and V (Bologna and Voinnet, 2014). After the siRNAs have been cleaved by DCL, they are loaded into AGRONAUTS (AGOs) and companies with a complexing gene silence machinery called RISC (RNA Induced Silence Complex). The RISC recognizes the complementary sequence of mRNA and AGO-loaded small RNA (also known as 'guide RNA'), then RISC suppresses the target mRNA via a cleavage or transcription gene silencing (TGS) mechanism. Small, interfering RNA is naturally very important in the organism to protect it from various natural enemies. For example, RNA interference (RNAi) was seen as a natural defense mechanism that used exogenous siRNAs to protect organisms from viruses, but it soon became clear that endogenous siRNAs (endo-siRNAs) also play a role in regulating genomic functions (Kamthan et al., 2015).

Piwi-interacting RNAs (piRNA)

Piwi-interacting RNAs are small non-coding RNAs that have 20-31nt. The name, piRNA (Piwi-interacting RNA), reflects the fact that piRNAs bind to Piwi proteins under physiological conditions. Piwi-interacting RNAs were first discovered in *Drosophila* as repeat-associated siRNAs (rasiRNA), which show complementarities to a variety of transposable and repetitive elements (Minna et al., 2011).

The main function of these RNA molecules involves chromatin regulation and suppression of transposon activity in germ-line and somatic cells. piRNAs are antisense to expressed transposons target and cleave the transposon in complexes with piwi proteins. This cleavage generates additional piRNAs which target and cleave additional transposons. This cycle continues to produce an abundance of piRNAs and augment transposon silencing (Lindsay et al., 2013).

Long non-coding RNA (lncRNA)

LncRNAs are transcripts generally longer than 200nt having little or no potential of encoding proteins. Most of the lncRNAs have similar characteristics within the mRNA, transcribed by RNA polymerase II. In addition to RNA Pol II-derived lncRNAs, there are other classes of lncRNAs transcribed by two plant-specific DNA-dependent RNA polymerases, RNA Pol IV and RNA Pol V, which play critical roles in transcriptional gene silencing mediated by RNA-dependent DNA methylation (RdDM) (Sang and Chanseok, 2016).

LncRNA can be divided based on genomic location; sense lncRNAs overlap with one or more exons of a transcript on the same strand; antisense lncRNAs overlap with one or more exons of a transcript on the opposite strand; intronic lncRNAs derive from an intron within another transcript; and intergenic lncRNAs occur in the interval between two genes on the same strand (Ma et al., 2013).

Although only a small number of lncRNAs are identified and functionally investigated until now, plant lncRNAs play important roles as regulators in complex gene regulatory networks involved in plant development and stress management (Zhang et al., 2014). The human genome has only 3% of the coding region but more than 85% of the genome is actively transcribed and the biggest challenge is the understanding of the functional role for these transcripts (Hangauer et al., 2013).

The lncRNA regulates the expression levels of target genes ranging from transcription to translation. Some examples of their functions are lncRNA, called LDMAR (for long-day specific male-fertility-associated RNA), which regulates the photoperiod-sensitive male sterility of the rice variety whose pollen is completely sterile in a long-day condition. Genome-wide investigation on rice also identified a set of lncRNAs that are specifically expressed during the reproduction stage (Zhang et al., 2014). On the Flowering Locus C (FLC) in *Arabidopsis*, an antisense lncRNA, COOLAIR, and a sense lncRNA, COLD AIR, are produced during vernalization to form an epigenetic switch for silencing the expression of the FLC gene to promote flowering (Fatica and Bozzoni, 2014, Renyi and Jiankang, 2014).

APPLICATION OF RNAi IN CROP IMPROVEMENT

Crop yield improvement is the ultimate goal of molecular

crop breeding. There are multiple physiological traits influencing crop yield, and several studies have found ncRNAs and their target genes to be involved in those traits. Some physiological traits which influence crop yield are plant manipulation, abiotic stress, biotic stress, and improvement in fruit quality, quantity, and nutritional value.

Plant architecture

Biomass

RNA interferences are one application that can improve the yield of crops and fruit vegetation via the manipulation of primary agronomic traits. It can increase the biomass of the crops and fruits by manipulation of plant height, prolonged vegetative segment and delayed flowering time, a number of branches or branching type, and measurement of the plants.

RNA interference knocks down the OsDWARF4 gene in rice to limit the plant's erect leaf and growing the photosynthesis through reducing leaves. The yield of such plants is improved or increased via dense planting conditions (Feldmann, 2006). Over-expression of the maize MIR156, Corngrass1 (Cg1) gene (Chuck et al., 2011), and red clover (*Trifolium pratense* L.) (Zheng et al., 2016) motives prolong the vegetative parts of maize and delayed flowering. This means that the reproductive stage is delayed, the vegetative parts are increased in size, and at the identical time, biomass of plants become increasing.

Moderate and low ranges of miR156 expression had 58–101% more biomass production than wild-type controls because of increases in tiller numbers in change grass plants. Over-expression of rice miR156 should improve the yield of solubilized sugar as properly as forage digestibility (Xie et al., 2012, Johnson, 2017), suspending the flowering time in the Arabidopsis (Roussin et al., 2020), and it can manipulate the white and lily flowering colors (Yamagishi and Sakai, 2020).

Grain yield

Improvements of the plants by way of special technology or techniques are mainly for increasing the yield of the crops. RNA interferences are one of the technologies which are used to improve the crop's yield by using manipulating traits. One of the functions of RNA interferences is the manipulation of the gene, which affects the characteristics of the crop whether to be increasing or reducing the crop yield.

Regulatory ncRNAs influence the reproductive stage. It is a very important aspect that affects crop yield and is used for genomic association. According to Ding et al. (2019), lncRNA, called LDMAR (for LONG-DAYSPECIFIC MALE-FERTILITY-ASSOCIATED RNA), regulates the photoperiod sensitive male sterility of rice with absolutely sterile pollen in a long-day condition. Genome-wide investigation on rice additionally identified a set of lncRNAs that are particularly expressed during the reproduction stage (Zhang et al., 2014).

The RNA mediates suppression of GA 20-oxidase (OsGA20ox2) gene which resulted in semi-dwarf plant life from a taller rice variety QX1. It increases panicle length, the quantity of seeds per panicle, and greater seed weight. OsSPL14 (Souamosa promoter binding protein-like14) is the goal of Osa-miR156 in rice to increase the yield of the rice grain, reduced tiller number, and accelerated grain yield (Wang et al., 2012; Jiao et al., 2010). Overexpression of Osa-miR1873 also resulted in some defects in yield traits, which include grain numbers and seed putting rate in rice (Zhou et al., 2020). Overexpression of the OsAGO17 gene was once also found to be involved in increased grain size, weight, and promote stem development in rice (Zhong et al., 2020).

Fruit improvement

The application of transgenic protects crops from different pests that can affect the plant products. Genetic engineering can be applied to improve the composition and quality of the harvested organs to reduce post-harvest deterioration of fruits or increase agronomic quality and nutritional value. Fruits are consumed when fresh because they are very sensitive to pests and are perishable. RNA interference is the technology that can overcome this problem (Meli et al., 2010).

Enhanced nutritional value and edibility

RNA silencing-based technology has been used in improving the nutritional value of crops. By down-regulating key genes in plant metabolic pathways usage of RNAi constructs, transgenic plants may also accumulate more favorable metabolites or produce fewer undesirable ingredients. Crops have exclusive nutritional values; some of them are allergens to human being, some pollutants to the environments, and some allergens to the different crops. But there are plants which have very essential nutritional values that are consumed by means of human beings or animals. RNA interference is to manipulate all these nutrients through adding the essential one and removing the unwanted ones.

Tomato (*Lycopersicon esculentum*) is one of the most economically essential fruit plants throughout the world rich in antioxidants, minerals, fibers, and vitamins. RNAi has been utilized in the development of tomato fruit with

an improved level of carotenoids and flavonoids which are especially beneficial for human health (Kamthan et al., 2015).

RNAi approach has additionally been used in apple to improve the fruit quality via enhancing self-life and reducing the quantity of a major apple allergen, metabolites, and accumulation of sugars in the fruits through sorbitol synthesis, which impacts fruit starch accumulation (Romer et al., 2020) and sugar-acid stability (Teo et al., 2006).

Some examples of nutrition adding plants through RNAi are high lysine maize for the expression of zein proteins (Li and Song, 2020; Choudhary et al., 2021), and silencing of carotenoid β-hydroxylases which increases the β-carotene content of maize (Berman et al., 2017).

RNAi has also been used to down-regulate the starch-branching enzyme resulting in high- amylose wheat, which has an amazing potential to improve human health (Man and Hong, 2013). Corn with increased essential amino acids (Hasan and Rima, 2021), improved soybean by using oil quality (Yang et al., 2018), and cotton with improved fatty acid composition have been developed with the use of RNAi. Overexpression of GmPDAT genes elevated seed size and oil content (Gao et al., 2020), whereas RNAi strains had reduced seed size and oil content of soybean (Liu et al., 2020). Suppression of three carotenoid-cleavage dioxygenase genes, OsCCD1, 4a, and 4b, increases carotenoid content in rice (Ko et al., 2018).

Enhanced shelf life

The fundamental issues of fruits are post-harvest deterioration and spoilage. It is a main financial loss. This may be because of some issues like; technique of harvesting, transports, and storage. Therefore, an increase in the shelf life of vegetables and fruits through delayed ripening involves any other critical agronomic trait that is being addressed through non-coding RNA technology. Initiation of ripening in climacteric fruits like tomato is characterized through a climacteric burst of ethylene, resulting in the regulation of the expression of ripening-specific genes. Manipulating the gene which is accountable to produce ethylene and decrease the production of ethylene was once increasing the shelf life of tomato (Osorio et al., 2011). RNA interference decreases the expression of 1-aminocyclopropane-1-carboxylate (ACC) oxidase, a gene of the ethylene biosynthesis pathway in tomato, and inhibited the ethylene production at the ripening time so that the fruit can survive a long time.

RNA silencing used to be first genetically modified in the Flavr Savr tomato, bringing about the antisense of transcript polygalacturonase (PG) which is suppressed to PG expression. The polygalacturonase is accountable for cell wall degradation during tomato ripening. Suppression of polygalacturonase delayed the natural softening of tomatoes and allowed tomatoes to ripen on the vine for long and resulting in a greater flavorful fruit (Renyi and Jiankang, 2014). The increase in shelf life of tomatoes used to be observed after increasing abscisic acid (ABA) content. Manipulation of β-carotene stages results in an enchantment that is no longer only limited to the shelf life of tomatoes, but also their nutritional value (Diretto et al., 2020).

Tomato fruits are considered to be climacteric and require the gaseous hormone ethylene to ripen. In every case, the change of the expression of the mi156 gene in tomatoes led to an increase in yield and shelf life (Zhang et al., 2011). Definitely, tomato has emerged as the pre-eminent experimental model for studying fleshy fruit, which includes the developmental control of ripening, ethylene synthesis and perception. Overexpression of Pti4, Pti5, and Pti6 genes (Wang et al., 2021), and SlGRAS4 gene (Liu et al., 2021a) in tomato are very crucial to accelerated fruit ripening and elevated the complete carotenoid content.

Non-coding RNA is especially primary within the increased shelf life of vegetables and fruits. Tobacco (Moreno et al., 2020), and tomatoes (Arefin et al., 2020), superoxide dismutase (SOD) genes expressed at some stage in the ripening of apple fruit (Lv et al., 2020), cold storage responses genes in the peach (Antonella et al., 2020), blueberry cultivars with higher fruit firmness and longer shelf lifestyles (Liu et al., 2021), preserved post-harvest shelf life and quality of banana fruit (Yumbya et al., 2021) have been developed using RNAi. RNAi method concentrated on suppression of more than one homolog would be much effective than the knockdown of a single homolog (Gupta et al., 2013).

Seedless fruit development (Parthenocarpy)

Parthenocarpy or seedless fruit improvement is a technique of fruit production from seedless crops by way of ovaries without pollination and fertilization. Parthenocarpy or seedlessness is a highly preferred agronomic trait, particularly in safe to eat fruit crops. It produces high yields in harsh environmental conditions, as no pollination or fertilization is required. Customers constantly want fresh fruit, while it is possible to produce the fruit at any time of the year. It produces excessive yields in harsh environmental conditions, as no pollination or fertilization is required. Customers continually want clean fruit, while it is possible to produce the fruit at any time of the year.

In some cases, fruits produce hard seed which makes it difficult to overcome the dormancy of the seed, whereas others produce seeds with the difficult tests, as the absence of seeds can also be a positive trait for both

direct clean consumption (e.g. grape, citrus, and banana) and industrial approaches (e.g. frozen eggplants, and tomato sauce) (Meli et al., 2010).

RNA interferers are one of the most essential primary technologies for overcoming the issues of vegetation with parthenocarpy. Some plants can move forward through RNAi innovation like; manipulation of auxin response factors8 (ARF8), which is the goal of miR167 to affect product from parthenocarpic fruits in each arabidopsis and tomatoes (Molesini, et al., 2012). Suppression of the orthologous genes of Pad-1 caused parthenocarpic fruit improvement in Solanaceae plants; hence, it is a very powerful tool in improving Solanaceae fruit production (Matsuo et al., 2020).

The overexpression of the PbGA20ox2 gene modified the GA biosynthetic pathway and improved GA4 synthesis, which promoted fruit set and parthenocarpic fruit improvement in pear fruits (Pyrus Bretschneider Rehd.) (Wang et al., 2020a). The PpIAA19 gene used to be concerned in the regulation of lateral root number, stem elongation, parthenocarpy, and fruit structure of tomatoes (Ding et al., 2019) and grapevines (Wang et al., 2020a). The overexpression of the MaTPD1A gene in banana plants produces seedless fruits in contrast to wild-type plants (Hu et al., 2020).

Biotic stress resistance

Phyto-pathogens are disease causing agents that can affect crops and crop products. The disease may affect the crop at different stages, seedling, vegetative, and at productive stages. RNAi strategies have been employed to improve the small RNA-mediated crop improvement defense mechanism in crop plants against various biotic stresses including an attack by viruses, bacteria, fungi, nematodes, and insects (Park and Shin, 2015).

Virus resistance

Viruses are pathogens that can influence crop products. RNA interference is one of the technologies which can overcome their effect. The functions of RNA interferences are protection mechanism of virus that invades nucleic acid molecules. Transgenic plant technology has been used to express genes encoding viral coat proteins in transgenic plants and can be resistant to viruses containing the coat proteins. The virus resistance was primarily based on the recognition of coat proteins through the transgenic plant cells and therefore on the plant immune response against the coat proteins. However, for understanding the application of genetic transformation technology, the plants can express the coat protein gene transcript and damage the protein coat; however, it cannot produce the protein that acts against the protein coat itself. Transgenic plants that are resistant to viruses have been produced by way of sense transgene-triggered RNAi against the viral RNAs (Ding, 2010; Renyi and Jian-Kang, 2014; Bahadur et al., 2015; Uslu and Wassenegger, 2020).

RNAi has shown a way to keep virus-resistant traits in many crops. The transgenic plant can produce the viral sequences that match coat proteins, replication-associated proteins, ATPases, or promoter areas in the viral genomes that can derive transgenic siRNAs to goal viral RNAs for degradation upon infection. Plants reportedly consisting of virus resistance included some suggested crops like papaya (Kertbundit et al., 2007), cassava (Vanitharani et al., 2004; Vanderschuren et al., 2012) and potato (Sajid et al., 2019). Some examples are potato resistance to spindle tuber viroid (PSTVd) and cassava resistance to African Cassava Mosaic Virus (ACMV) (Renyi and Jiankang, 2014). The virus prevention strategies are based totally on the ecological implication that increased carbon dioxide concentrations minimize the accumulation of the cucumber mosaic virus in *Nicotiana tabacum* through the viral suppressor of the RNAi (VSR) 2b protein of CMV (Guo et al., 2021).

Bacterial resistance

Bacterial diseases are extremely hard to manage due to the high rate of production of the spread. The multiplication rates of microorganism are very excessive in contrast to plant production, due to which, it can effortlessly manage plant development. RNA interference application technologies are used in various facilities to resist bacterial diseases. Some plants that can withstand RNA interference are; In Arabidopsis, it was reported that miR393 is caused through a bacterial pattern-associated molecular pattern (PAMP) peptide flg22 and negatively regulates the F-box auxin receptors TIR1, AFB2, and AFB3. This suppression of auxin signaling contributed positively to the predicament of bacterial infection (*Pseudomonas syringae*) (Li et al., 2010; Zhang et al., 2011a). The other application RNAi mediated the suppression of two genes from *Agrobacterium tumefaciens* that are involved in the formation of crown gall tumors (iaaM and ipt), which could appreciably minimize tumor production in Arabidopsis (Kamthan et al., 2015).

Overexpression of the rice chorismate mutase (OsCM) gene modified the downstream pathway of the aromatic amino acids, whereby the stress of bacterial leaf rot (BLB) was weakened through changing stress-sensitive genes and hormonal accumulation (Jan et al., 2020). Some of the well-reported plants that showed bacteria can be resisted through manipulating RNAi genes include tomatoes (Bento et al., 2020), citrus (Yu and Killiny, 2020), soybean (Tian et al., 2020), and Arabidopsis (Guo et al., 2020).

Fungal resistance

Genetic engineering based on RNA silencing has made a primary contribution to improving crops, that is, resistance to pathogens. Fungus is a pathogen that can affect plant production and quality. RNAi has been confirmed to be an essential strategy for producing tolerance in various crops (Kamthan et al., 2015).

RNA interference is done in response to fungal attack in wheat *Blumeria graminis* f. Sp. tritici (Bgt) through the use of the 24 miRNAs gene that causes devastating diseases of wheat powdery mildew (Xin et al., 2010). Transgenic overexpression of rice plants through OSA-miR7695 (Campo et al., 2013), miR160a or miR398b (Li et al., 2014), miR169 (Li et al., 2017) and OsamiR167d (Zhao et al., 2020) has been negatively regulated as a response to the blast fungus Magnaportheoryzae, and through overexpression of these genes, an improved resistance against rice blast infections was achieved.

Treating of the *Fusarium* species with various dsRNAs that concentrated on the genes was destructive to the fungus and leads to determination of an extended growth in *in vitro* cultures (Koch et al., 2018). In the reduction of the *Arabidopsis thaliana* line, it was observed that the activity of miR396 confers resistance to necrotrophic and hemibiotrophic fungal pathogens using artificial miRNA goal mimetics (Soto-Suárez et al., 2017). Overexpression of the BnaNPR1 gene in oilseed rape played a high-quality role in the resistance of *Brassica napus* to *Sclerotinia sclerotiorum*, which confers resistance to this pathogen (Wang et al., 2020b).

Insect and resistance

Defoliation of plants or sucking out their sap insects can cause great damage to plants by slowing, weakening, and sometimes killing their increase (Bahadur et al., 2015). The use of RNAi has been confirmed to be an essential approach for developing tolerance in various plants. Insect-resistant plants produce the dsRNA that attacks the insects, and when insects ingest, the gene expresses itself (Huvenne and Smagghe, 2010).

This technology is intended to protect insects from various kinds of plant production; among others, the western corn rootworm *Diabrotica virgifera*, the cotton bollworm *Helicoverpa armigera*, and the tobacco hawk *Manduca sexta* (Renyi and Jian-kang, 2014). Transgenic tobacco lines expressing dsRNA of v-ATPase and leading to whitefly mortality rate (Thakur et al., 2014) transcript level of goal genes in *Bemisia tabaci* at more than 70% mortality was observed (Raza et al., 2016; Shelby et al., 2020).

The knockdown of CsKrh1 mediated through RNA interference substantially decreased the transcription of vitellogenesis (Vg) within *C. suppressalis*, which is extremely essential in the suppression of rice pests (Tang et al., 2020). For pest management in the field through topical application or spraying, dsRNA shows a very high potential, with soybean aphids *Aphis glycines* (Yan et al., 2020a) mortality of up to 81.67% and with soybean *Nezara viridula* mortality of up to 90% recorded (Sharma et al., 2021).

Abiotic stress tolerance

Plant growth in the field can be exposed to several abiotic stresses, such as: drought, salt, heat and cold. RNA silencing coding is one of the technologies that can overcome this problem, the abiotic stress of plant products. By regulating the endogenous level of regulatory ncRNAs in response to abiotic stress, they regulate the expression of their target genes, which are closely involved in specific or multiple stresses.

Drought and salinity tolerance

Lack of water or drought and salinity are the abiotic stresses that are the main environmental stresses that restricts crop productivity. RNA silencing coding has been used successfully to enhance drought and salt tolerance cultures. RNA interference is used in oilseed rape to supply the AtHPR1 promoter, which is resistant to seed break-off during drought-induced flowering, besides affecting yield in drought stress. Transgenic rice plants that are drought stress-tolerant have been developed such as the receptor for activated C-kinase1 (RACK1) (Li et al., 2009), knockdown of a RING finger E3 ligase gene OsDSG1, and also silencing OsDIS1 for the drought-induced SINA protein through *Oryza sativa* (Park et al., 2010).

A wide variety of miRNAs has been recognized in *Brassica* that responds to drought, high salinity, and stress at high temperatures. Of 126 newly recognized miRNAs, miR164, miR160, and miR156 were experimentally approved to goal NAC domain-containing proteins, ARF17-like, and SPL2-like proteins, respectively (Bhardwaj et al., 2014).

However, the RNA interference has also regulated the gene to respond in an identical way to the salinity tolerance plants. The overexpression of GmNFYA3 in Arabidopsis led to an increased sensitivity to salinity stress, and exogenous ABA (Ni et al., 2013) as well as transgenic creeping bentgrass (*Agrostis stolonifera*) plants that overexpressed a rice miR319 gene (OsamiR319) also confirmed an increased tolerance to drought and salinity related with increased leaf wax content and water retention; however, there was decreased sodium intake (Zhou and Luo, 2013). In

tomato, overexpression of the miR169c gene led to a reduction in stoma openings, the transpiration rate, and the loss of leaf water, which improved the drought tolerance in transgenic plants compared to wild-type controls (Zhang et al., 2011a). Accordingly, a knockdown of the OsTBP2.2 gene was generated in rice in order to increase rice sensitivity to drought stress (Zhang et al., 2020).

Cold and heat stress tolerance

Cold and heat are the abiotic types of stress that can influence plant production. With the variable conditions, the plants are pale; also, the yield and quality of plant products decrease and additionally affects the financial loss. Transgenic plants that use RNA silencing coding can overcome the problem of this stress. It has been suggested that miR319 expression changes in response to cold stress in Arabidopsis, rice, and sugar cane (Lv et al., 2020).

The overexpression of the Osa miR319 gene led to increased cold stress tolerance (4C) after cold acclimatization (12C) of plants (Yang et al., 2013). In rice, the overexpression of OsPCF5 and OsTCP21 led to the production of the cold-resistant transgenic plant (Yang et al., 2013).

Guan et al. (2013) observed a new kind of plant thermotolerance mechanism, in particular to protect the reproductive organs. It includes the induction of miR398 to downregulate its goal genes CSD (copper / zinc superoxide dismutase), CSD1 and CSD2, and CCS (a gene that codes for copper chaperones for CSD1 and CSD2). They observed that csd1, csd2 and ccsmutanten showed a higher heat stress tolerance than wild-type plants, combined with an increased accumulation of heat stress transcription factors and heat shock proteins as well as much less damage to plants (Guan et al., 2013). Corn (Yu et al., 2018) and cassava (Suksamran et al., 2020) responds to abiotic stress such as heat, cold, salt, and drought.

CONCLUSION

One of the basic requirements of a human being is food. However, food insecurity and malnutrition are currently among the most serious concerns for human health, causing the loss of countless lives in developing countries. Therefore, there is need for an innovative technology to improve upon our crop production methods and practices. RNA silencing gene is an advanced application that can solve the agricultural problem in a short period. In crop improvement, it has a wider application in the production of transgenic plants, which have improved yield, increased nutritional qualities with improved taste, texture or appearance, and health benefits. It also enables us to produce plants that have reduced dependence on fertilizers, pesticides, and other agrochemicals, and plants which have reduced the vulnerability of crops to environmental stresses. RNA interference applications are innovative technologies that can contribute to the solution to these problems. It describes several mechanistically related pathways which are involved in controlling and regulating gene expression. RNA silencing pathways are associated with the regulatory activity of non-coding RNAs that function as factors involved in inactivating homologous sequences, promoting endonuclease activity, translational arrest, and/or chromatic or DNA modification. It also has some limitations which include identification of appropriate target genes, off-target effects, and the application of RNAi is more sophisticated and needs highly skilled human power.

CONFLICT OF INTERESTS

The author has not declared any conflict of interests.

REFERENCES

Anita QG, Sofia N, Helena S (2013). Non-Coding RNAs: Multi-Tasking Molecules in the Cell. International Journal of Molecular Sciences 14:16010-16039

Antonella M, Muller CT, Bruno L, McGregor L, Ferrante A, Ceverista CAA, Spadafora ND (2020). Fruit volatile profiling through GC× GC-ToF-MS and gene expression analyses reveal differences amongst peach cultivars in their response to cold storage. Scientific Reports (Nature Publisher Group) 10(1).

Arefin P, Amin R, Sadiq MZA, Dey SS, Boby F, Parvaz MS (2020). A Study of Effectiveness of Natural Coatings on the Shelf Life Extension of Tomatoes by the Observation of TomloxC Gene Expression. Bioscience Biotechnology Research Asia 17(3):459-465.

Bader AS, Hawley BR, Wilczynska A, Bushell M (2020). The roles of RNA in DNA double strand break repair. British Journal of Cancer 122(5):613-623.

Bahadur B, Rajam MV, Sahijram L, Krishnamurthy KV (2015). Induced mutations and crop improvement. Plant Biology and Biotechnology 1(23):593-617.

Bento FM, Marques RN, Campana FB, Demétrio CG, Leandro RA, Parra JRP, Figueira A (2020). Gene silencing by RNAi via oral delivery of dsRNA by bacteria in the South American tomato pinworm, Tuta absoluta. Pest Management Science 76(1):287-295.

Berman J, Zorrilla-López U, Sandmann G, Capell T, Christou P, Zhu C (2017). The silencing of carotenoid β-hydroxylases by RNA interference in different maize genetic backgrounds increases the β-carotene content of the endosperm. International Journal of Molecular Sciences 18(12):2515.

Bhardwaj AR, Joshi G, Pandey R, Kukreja B, Goel S, Jagannath A, Agarwal M (2014). A genome-wide perspective of miRNA ome in response to high temperature, salinity, and drought stresses in *Brassica juncea* (Czern) L. Plos One 9(3):92456.

Bologna NG, Voinnet O (2014). The diversity, biogenesis, and activities of endogenous silencing small RNAs in *Arabidopsis*. Annual Review of Plant Biology 65:473-503

Brant EJ, Budak H (2018). Plant small non-coding RNAs and their roles in biotic stresses. Frontiers in Plant Science 9:1038.

Campo S, Peris-Peris C, Sire C, Moreno AB, Donaire L, Zytnicki M (2013). Identification of a novel microRNA (miRNA) from rice that targets an alternatively spliced transcript of the Nramp6 (Natural resistance-associated macrophage protein6) gene involved in pathogen resistance. New Phytologist 199(1):212-227.
Choudhary M, Grover K, Singh M (2021). Maize's significance in the Indian food situation to mitigate malnutrition. Cereal Chemistry 98(2):212-221.
Chuck GS, Tobias C, Sun L, Kraemer F, Li C, Dibble D (2011). Overexpression of the maize corn grass1 microRNA prevents flowering, improves digestibility, and increases the starch content of switchgrass. Proceedings of the National Academy of Sciences, 108(42):17550-17555.
Crick F (1970). Central dogma of molecular biology. Nature 227:561-563.
Ding SW (2010). RNA based antiviral immunity. Nature Reviews Immunology 10:632-644.
Ding Y, Zeng W, Wang X, Wang Y, Niu L, Pan L, Wang Z (2019). Over- expression of Peach PpIAA19 in Tomato Alters Plant Growth, Parthenocarpy and Fruit Shape. Journal of Plant Growth Regulation 38(1):103-112.
Diretto G, Frusciante S, Fabbri C, Schauer N, Busta L, Wang Z, Giuliano G (2020). Manipulation of β-carotene levels in tomato fruits results in increased ABA content and extended shelf life. Plant Biotechnology Journal 18(5):1185-1199.
Fatica A, Bozzoni I (2014). Long non-coding RNAs: new players in cell differentiation and development. Nature Reviews Genetics 15:7-21.
Feldmann KA (2006). Steroid regulation improves crop yield. Nature Biotechnology 24:46-47.
Gao L, Chen W, Xu X, Zhang J, Singh TK, Liu S, Liu Q (2020). Engineering Trienoic Fatty Acids into Cottonseed Oil Improves Low-Temperature Seed Germination, Plant Photosynthesis and Cotton Fiber Quality. Plant and Cell Physiology 61(7):1335-1347.
Guan Q, Lu X, Zeng H, Zhang Y, Zhu J (2013). Heat stress induction of miR398 triggers a regulatory loop that is critical for thermo-tolerance in *Arabidopsis*. Plant Journal 74(5):840-851.
Guo H, Ge P, Tong J, Zhang Y, Peng X, Zhao Z, Sun Y (2021). Elevated Carbon Dioxide Levels Decreases Cucumber Mosaic Virus Accumulation in Correlation with Greater Accumulation of rgs-CaM, an Inhibitor of a Viral Suppressor of RNAi. Plants 10(1):59.
Guo W, Chen W, Zhang Z, Guo N, Liu L, Ma Y, Dai H (2020). The hawthorn CpLRR-RLK1 gene targeted by ACLSV-derived vsiRNA positively regulates resistance to bacteria disease. Plant Science 300:110641.
Gupta A, Pal RK, Rajama M (2013). Delayed ripening and improved fruit processing quality in tomatoes by RNAi-mediated silencing of three homologs of 1- aminopropane-1-carboxylate synthase gene. Journal of Plant Physiology 170(11):987-995.
Hangauer MJ, Vaughn IW, McManus MT (2013). Pervasive transcription of the human genome produces thousands of previously unidentified long intergenic noncoding RNAs. PLoS genetics 9(6):e1003569.
Hasan MM, Rima R (2021). Genetic engineering to improve essential and conditionally essential amino acids in maize: transporter engineering as a reference. Transgenic Research 30(2):207-220.
Hu C, Sheng O, Dong T, Yang Q, Dou T, Li C, Bi F (2020). Overexpression of MaTPD1A impairs fruit and pollen development by modulating some regulators in Musa itinerant. BMC Plant Biology 20(1):1-12.
Huvenne H, Smagghe G (2010). Mechanisms of dsRNA uptake in insects and potential of RNAi for pest control: a review. Journal of Insect Physiology 56(3):227-235.
Jan R, Khan MA, Asaf S, Lee IJ, Bae JS, Kim KM (2020). Overexpression of OsCM alleviates BLB stress via phytohormonal accumulation and transcriptional modulation of defense-related genes in *Oryza sativa*. Scientific reports 10(1):1-15.
Jiao Y, Wang Y, Xue D, Wang J, Yan M, Liu G, Dong G, Zeng D, Lu Z, Zhu X, Qian Q, Li J (2010). The regulation of OsSPL14 by OsmiR156 defines the ideal plant architecture in rice. Nature Genetics 42(6):541-544.
Johnson CR (2017). Reproduction and confinement of miR156 transgenic switchgrass (*Panicum virgatum* L.). https://trace.tennessee.edu/cgi/viewcontent.cgi?article=5844&context=utk_gradthes
Kamthan A, Chaudhuri A, Kamthan M, Datta A (2015). Small RNAs in plants: recent development and application for crop improvement. Front. Plant Science 6:208-210.
Kertbundit S, Pongtanom N, Ruanjan P, Chantasingh D, Tanwanchai A, Panyim S, Juříček M (2007). Resistance of transgenic papaya plants to Papaya ring spot virus. Biologia Plantarum 51(2):333-339.
Khraiwesh B, Zhu JK, Zhu J (2012). Role of miRNAs and siRNAs in biotic and abiotic stress responses of plants. Biochimica et Biophysica Acta 1819(2):137-148.
Ko MR, Song MH, Kim JK, Baek SA, You MK, Lim SH, Ha SH (2018). RNAi-mediated suppression of three carotenoid-cleavage dioxygenase genes, OsCCD1, 4a, and 4b, increases carotenoid content in rice. Journal of Experimental Botany 69(21):5105-5116.
Koch A, Stein E, Kogel KH (2018). RNA-based disease control as a complementary measure to fight Fusarium fungi through silencing of the azole target Cytochrome P450 Lanosterol C-14 α-Demethylase. European Journal of Plant Pathology 152(4):1003-1010.
Li C, Song R (2020). The regulation of zein biosynthesis in maize endosperm. Theoretical and Applied Genetics 133(5):1443-1453.
Li DH, Hui LIU, Yang YL, Zhen PP, Liang JS (2009). Down-regulated expression of RACK1 gene by RNA interference enhances drought tolerance in rice. Rice Science 16(1):14-20.
Li Y, Lu YG, Shi Y, Wu L, Xu YJ, Huang F, Wang WM (2014). Multiple rice microRNAs are involved in immunity against the blast fungus *Magnaporthe oryzae*. Plant Physiology 164(2):1077-1092.
Li Y, Zhang Q, Zhang J, Wu L, Qi Y, Zhou JM (2010). Identification of microRNAs involved in pathogen-associated molecular pattern-triggered plant innate immunity. Plant Physiology 152(4):2222-2231.
Li Y, Zhao SL, Li JL, Hu XH, Wang H, Cao XL, Wang WM (2017). Osa-miR169 negatively regulates rice immunity against the blast fungus *Magnaporthe oryzae*. Frontiers in Plant Science 8:2.
Lindsay MA, Griffiths-Jones S, Sato K, Siomi MC (2013). Piwi-interacting RNAs: biological functions and biogenesis. Essays in Biochemistry 54:39-52.
Liu JY, Zhang YW, Han X, Zuo JF, Zhang Z, Shang H, Zhang YM (2020). An evolutionary population structure model reveals pleiotropic effects of GmPDAT for traits related to seed size and oil content in soybean. Journal of Experimental Botany 71(22):6988-7002.
Liu Y, Shi Y, Su D, Lu W, Li Z (2021). SlGRAS4 accelerates fruit ripening by regulating ethylene biosynthesis genes and SlMADS1 in tomatoes. Horticulture Research 8(1):1-11.
Liu Y, Wang Y, Pei J, Li Y, Sun H (2021a). Genome-wide identification and characterization of the COMT gene family during the development of blueberry fruit. BMC Plant Biology 21(1):1-16.
Lv J, Zhang J, Han X, Bai L, Xu D, Ding S, Li J (2020). Genome-wide identification of superoxide dismutase (SOD) genes and their expression profiles under 1- methyl cyclopropane (1-MCP) treatment during the ripening of apple fruit. Scientia Horticulturae 271:109471.
Ma L, Bajic VB, Zhang Z (2013). On the classification of long non-coding RNAs. RNA Biology 10(6):925-933.
Man Z, Hong L (2013). MicroRNA-mediated gene regulation: potential applications for plant genetic engineering. Plant Molecular Biology 83(1-2):59-75.
Matsuo S, Miyatake K, Endo M, Urashimo S, Kawanishi T, Negoro S, Fukuoka H (2020). Loss of function of the Pad-1 aminotransferase gene, which is involved in auxin homeostasis, induces parthenocarpy in Solanaceae plants. Proceedings of the National Academy of Sciences 117(23):12784-12790.
Meli VS, Ghosh S, Prabha TN, Chakraborty N, Chakraborty S, Datta A (2010). Enhancement of fruit shelf life by suppressing N-

glycan processing enzymes. Proceedings of the National Academy of Sciences of the United States of America 107(6):2413-2418.
Mezzetti B, Smagghe G, Arpaia S, Christiaens O, Dietz-Pfeilstetter A, Jones H, Sweet J (2020). RNAi: What is its position in agriculture? Journal of Pest Science 93:1125-1130.
Minna UK, Michael TYL, Christopher KG (2011). Non-coding RNAs as regulators of gene expression and epigenetics. Cardiovascular Research 90(3):430-440.
Molesini B, Youry P, Tiziana P (2012). Fruit improvement using intragenesis and artificial microRNA. Trends in Biotechnology 30:2.
Moreno JC, Mi J, Agrawal S, Kössler S, Turečková V, Tarkowská D, Schöttler MA (2020). Expression of a carotenogenic gene allows faster biomass production by redesigning plant architecture and improving photosynthetic efficiency in tobacco. The Plant Journal 103(6):1967-1984.
Ni Z, Hu Z, Jiang Q, Zhang H (2013). GmNFYA3, a target gene of miR169, is a positive regulator of plant tolerance to drought stress. Plant Molecular Biology 82(1-2):113-129.
Osorio S, Alba R, Damasceno CM, Lopez-Casado G, Lohse M, Zanor MI (2011). Systems biology of tomato fruit development: combined tran- script, protein, and metabolite analysis of tomato transcription factor and ethylene receptor (Nr) mutants reveals novel regulatory interactions. Plant Physiology 157(1):405-425.
Park GG, Park JJ, Yoon J, Yu SN, An G (2010). A RING finger E3 ligase gene, *Oryza sativa* Delayed Seed Germination 1 (OsDSG1), controls seed germination and stress responses in rice. Plant Molecular Biology 74(45):467-478.
Park JH, Shin C (2015). The role of plant small RNAs in NB-LRR regulation. Briefings in Functional Genomics 14:268-274.
Raza A, Malik HJ, Shafiq M, Amin I, Scheffler JA, Scheffler BE, et al (2016). RNA Interference based Approach to Down Regulate Osmoregulators of Whitefly (*Bemisia tabaci*): Potential Technology for the Control of Whitefly. PLoS ONE 11(4):e0153883.
Renyi L, Jiankang Z (2014). Non-coding RNAs as potent tools for crop improvement. National Science Review 1(2):186-189.
Rodnina MV, Wintermeyer W (2011). The ribosome as a molecular machine: the mechanism of tRNA–mRNA movement in translocation. Biochemical Society Transactions 39(2):658-662.
Romer E, Chebib S, Bergmann KC, Plate K, Becker S, Ludwig C, Schwab W (2020). Tiered approach for the identification of Mal d 1 reduced, well tolerated apple genotypes. Scientific Reports 10(1):1-13.
Roussin-Léveillée C, Silva-Martins G, Moffett P (2020). ARGONAUTE5 represses age- dependent induction of flowering through physical and functional interaction with miR156 in Arabidopsis. Plant and Cell Physiology 61(5):957-966.
Sajid IA, Tabassum B, Yousaf I, Khan A, Adeyinka OS, Shahid N, Husnain T (2019). In vivo gene silencing of potato virus X by small interference RNAs in transgenic potato. Potato Research 1:13. https://doi.org/10.1007/s11540-019-09433-0
Sang YS, Chanseok S (2016). Regulatory non-coding RNAs in plants: potential gene resources for the improvement of agricultural traits. Plant Biotechnology Reports 10(2):35-47.
Santosh B, Akhil V, Pramod KY (2014). Non-coding RNAs: biological functions and applications. Cell Biochemistry & Function 33(1):14-22.
Sharma R, Christiaens O, Taning CN, Smagghe G (2021). RNAi-mediated mortality in southern green stinkbug Nezara viridula by oral delivery of dsRNA. Pest Management Science 77(1):77-84.
Sharp SJ, Schaack J, Cooley L, Burke DJ, Soll D (1985). Structure and Transcription of Eukaryotic tRNA Genes. CRC Critical Reviews in Biochemistry 19(2):107-144.
Shelby EA, Moss JB, Andreason SA, Simmons AM, Moore AJ, Moore PJ (2020). Debugging: Strategies and Considerations for Efficient RNAi-Mediated Control of the Whitefly Bemisia tabaci. Insects 11(11):723.
Soto-Suárez M, Baldrich P, Weigel D, Rubio-Somoza I, San Segundo B (2017). The Arabidopsis miR396 mediates pathogen-associated molecular pattern-triggered immune responses against fungal pathogens. Scientific reports 7(1):1-14.
Suksamran R, Saithong T, Thammarongtham C, Kalapanulak S (2020). Genomic and transcriptomic analysis identified novel putative cassava lncRNAs involved in cold and drought stress. Genes 11(4):366.
Tang Y, He H, Qu X, Cai Y, Ding W, Qiu L, Li Y (2020). RNA interference- mediated knockdown of the transcription factor Krüppel homologue 1 suppresses vitellogenesis in Chilo suppressalis. Insect Molecular Biology 29(2):183-192.
Teo G, Suzuki Y, Uratsu SL, Lampinen B, Ormonde N, Hu WK, Dandekar AM (2006). Silencing leaf sorbitol synthesis alters long-distance partitioning and apple fruit quality. Proceedings of the National Academy of Sciences 103(49):18842-18847.
Thakur N, Upadhyay SK, Verma PC, Chandrashekar K, Tuli R, Singh PK (2014) Enhanced Whitefly Resistance in Transgenic Tobacco Plants Expressing Double Stranded RNA of *v-ATPase A* Gene. PLoS ONE 9(3):e87235.
Tian SN, Liu DD, Zhong CL, Xu HY, Yang S, Fang Y, Liu JZ (2020). Silencing GmFLS2 enhances the susceptibility of soybean to bacterial pathogen through attenuating the activation of GmMAPK signaling pathway. Plant Science 292:110386.
Uslu VV, Wassenegger M (2020). Critical view on RNA silencing-mediated virus resistance using exogenously applied RNA. Current Opinion in Virology 42:18-24.
Valle M, Zavialov A, Li W, Stagg SM, Sengupta J, Nielsen RC, Nissen P, Harvey SC, Ehrenberg M, Frank J (2003). Incorporation of aminoacyl-tRNA into the ribosome as seen by cryo-electron microscopy. Nature Structural Biology 10(11):899-906.
Vanderschuren H, Moreno I, Anjanappa RB, Zainuddin IM, Gruissem W (2012). Exploiting the combination of natural and genetically engineered resistance to cassava mosaic and cassava brown streak viruses impacting cassava production in Africa. PloS one 7(9):e45277.
Vanitharani R, Chellappan P, Pita JS, Fauquet CM (2004). Differential roles of AC2 and AC4 of cassava geminiviruses in mediating synergism and suppression of posttranscriptional gene silencing. Journal of Virology 78(17):9487-9498.
Wang C, Wang W, Abdelrahman M, Jiu S, Zheng T, Gong P, Fang J (2020a). Study on miRNAs-Mediated Seed and Stone-Hardening Regulatory Networks and the Mechanism of miRNAs' Manipulating Gibberellin-Induced Seedless Berries in Grapevine (*Vitis vinifera L.*). https://www.researchgate.net/publication/346804171_Study_on_miRNAs-Mediated_Seed_and_Stone-Hardening_Regulatory_Networks_and_the_Mechanism_of_miRNAs'_Manipulating_Gibberellin-Induced_Seedless_Berries_in_Grapevine_Vitis_vinifera_L
Wang Z, Zhang WH, Ma LY, Li X, Zhao FY, Tan XL (2020b). Overexpression of Brassica napus NPR1 enhances resistance to *Sclerotinia sclerotiorum* in oilseed rape. Physiological and Molecular Plant Pathology 110:101460.
Wang S,Wu K, Yuan Q, Liu X, Liu Z, Lin X, (2012). Control of grain size, shape and quality by OsSPL16 in rice. Nature Genetics 44:950-954.
Wang Y, Feng G, Zhang Z, Liu Y, Ma Y, Wang Y, Niu X (2021). Overexpression of Pti4, Pti5, and Pti6 in tomato promote plant defense and fruit ripening. Plant Science 302:110702.
Wheeler T, von Braun J (2013). Climate change impacts on global food security. Science 341:508-513.
Wilson RC, Doudna JA (2013). Molecular mechanisms of RNA interference. Annual Review of Biophysics 42:217-239.
Xie K, Shen J, Hou X, Yao J, Li X, Xiao J, Xiong L (2012). Gradual increase of miR156 regulates temporal expression changes of numerous genes during leaf development in rice. Plant Physiology 158(3):1382-1394
Xin M, Wang Y, Yao Y, Xie C, Peng H, Ni Z (2010). Diverse set of microRNAs are responsive to powdery mildew infection and heat stress in wheat (*Triticum aestivum* L.). BMC Plant Biology 10(1):123-134.
Yamagishi M, Sakai M (2020). The MicroRNA828/MYB12 Module Mediates Bicolor Pattern Development in Asiatic Hybrid Lily (*Lilium* spp.) Flowers. Frontiers in Plant Science 11.

Yan S, Qian J, Cai C, Ma Z, Li J, Yin M, Shen J (2020). Spray method application of transdermal dsRNA delivery system for efficient gene silencing and pest control on soybean aphid Aphis glycines. Journal of Pest Science 93(1):449-459.

Yan S, Ren B, Zeng B, Shen J (2020a). Improving RNAi efficiency for pest control in crop species. BioTechniques 68(5):283-290.

Yan S, Ren BY, Shen J (2021). Nanoparticle-mediated double-stranded RNA delivery system: A promising approach for sustainable pest management. Insect Science 28(1):21-34.

Yang C, Li D, Mao D, Liu X, Li C, Li X (2013). Over expression of microRNA319 impacts leaf morphogenesis and leads to enhanced cold tolerance in rice (*Oryza sativa* L.). Plant, Cell & Environment 36(12):2207-2218.

Yang J, Xing G, Niu L, He H, Guo D, Du Q, Yang X (2018). Improved oil quality in transgenic soybean seeds by RNAi-mediated knockdown of GmFAD2-1B. Transgenic Research 27(2):155-166.

Yu X, Killiny N (2020). RNA interference-mediated control of Asian citrus psyllid, the vector of the huanglongbing bacterial pathogen. Tropical Plant Pathology 45:298-305.

Yu X, Meng X, Liu Y, Li N, Zhang A, Wang TJ, Jiang L, Pang J, Zhao X, Qi X, Zhang M (2018). The chromatin remodeler ZmCHB101 impacts expression of osmotic stress-responsive genes in maize. Plant Molecular Biology 97(4):451-65.

Yumbya P, Ambuko J, Hutchinson M, Owino W, Juma J, Machuka E, Mutuku JM (2021). Transcriptome analysis to elucidate hexanal's mode of action in preserving the post-harvest shelf life and quality of banana fruits (*Musa acuminata*). Journal of Agriculture and Food Research 100114.

Zhang W, Gao S, Zhou X, Chellappan P, Chen Z, Zhou X, Zhang X, Fromuth N, Coutino G, Coffey M, Jin H (2011). Bacteria responsive microRNAs regulate plant innate immunity by modulating plant hormone networks. Plant Molecular Biology 75:93-105.

Zhang X, Zou Z, Zhang J, Zhang Y, Han Q, Hu T, (2011a). Over expression of sly- miR156a in tomato results in multiple vegetative and reproductive trait alterations and partial phenocopy of the sft mutant. FEBS Letters 585:435-439.

Zhang Y, Zhao L, Xiao H, Chew J, Xiang J, Qian K, Fan X (2020). Knockdown of a Novel Gene OsTBP2.2 Increases Sensitivity to Drought Stress in Rice. Genes 11(6):629.

Zhang YC, Liao JY, Li ZY, Yu Y, Zhang JP, Li QF, Qu LH, Shu W, Chen YQ (2014). Genome-wide screening and functional analysis identify a large number of long noncoding RNAs involved in the sexual reproduction of rice. Genome Biology 15:5-12.

Zhao ZX, Feng Q, Cao XL, Zhu Y, Wang H, Chandran V, Wang WM (2020). Osa-miR167d facilitates infection of Magnaporthe oryzae in rice. Journal of Integrative Plant Biology 62(5):702-715.

Zheng LL, Qu LH (2015). Application of microRNA gene resources in the improvement of agronomic traits in rice. Plant Biotechnology Journal 13:329-336.

Zheng Q, Liu J, Goff BM, Dinkins RD, Zhu H (2016). Genetic manipulation of miR156 for improvement of biomass production and forage quality in red clover. Crop Science 56(3):1199-1205.

Zhong J, He W, Peng Z, Zhang H, Li F, Yao J (2020). A putative AGO protein, OsAGO17, positively regulates grain size and grain weight through OsmiR397b in rice. Plant Biotechnology Journal 18(4):916-928.

Zhou M, Luo H (2013). MicroRNA-mediated gene regulation: potential applications for plant genetic engineering. Plant Molecular Biology 83:59-75.

Zhou SX, Zhu Y, Wang LF, Zheng YP, Chen JF, Li TT, Wang WM (2020). Osa-miR1873 fine-tunes rice immunity against Magnaporthe oryzae and yield traits. Journal of integrative plant biology 62(8):12213-1226.

Vol. 20(11), pp.451-464, November 2021
DOI: 10.5897/AJB2021.17359
Article Number: D26543268193
ISSN: 1684-5315

http://www.academicjournals.org/AJB

African Journal of Biotechnology

Full Length Research Paper

Statistical modeling of effective doses in hormetic dose-response relationships by reparameterization of a bilogistic model for inverted U-shaped curves

Christian O. Nweke[1*], Oluchukwu R. Nwangwu[1], Chukwudi J. Ogbonna[2] and Reuben N. Okechi[3]

[1]Department of Microbiology, Federal University of Technology Owerri, P.M.B. 1526, Owerri, Imo State, Nigeria.
[2]Department of Statistics, Federal University of Technology Owerri, P.M.B. 1526, Owerri, Imo State, Nigeria.
[3]Department of Biotechnology, Federal University of Technology Owerri, P.M.B. 1526, Owerri, Imo State, Nigeria.

Received 13 May 2021; Accepted 21 August 2021

Hormesis is a biphasic dose (concentration)-response phenomenon characterized by low dose stimulatory and high dose inhibitory effects exerted by stressors on living organisms. Recently, there has been increased interest in the phenomenon and statistical models for its exploration in toxicological studies. The bilogistic model of Beckon et al. is one of such models for modeling biphasic dose-response relationships in toxicological studies. However, there is no explicit formula for the estimation of effective doses (ED_K) with the model. In this study, a simple general approach was suggested to reparameterize the model, leading to a range of mathematical models for determination of effective doses at both stimulatory and inhibitory ranges in inverted U-shaped hormetic dose-response relationships. The reparameterized models were tested on experimental data from three different *in vitro* experimental systems obtained from literature and our experiment. They were successfully applied to test for significance of hormesis and estimate effective doses and their statistical properties. In addition, reparameterization of the model for a particular effective dose (ED_K) did not affect estimation of other parameters (such as x_1, x_2, β_1, β_2 and M). The reparameterized models provided useful tools for adequate exploration of the tested hormetic dose-response relationships. The extended models could hopefully be versatile in characterization of variable hormetic dose response relationships in many toxicological disciplines.

Key words: Toxicity, hormesis, hormesis quantities, model extension, concentration-responses.

INTRODUCTION

Hormesis is a dose-response relationship characterized by a low dose stimulation and high dose toxicity of a stressor. This phenomenon has been reawakened after a long period of marginalization and controversies. Hormesis has been reported to be generalizable, occurring in all forms of organisms for many endpoints and induced by physical and chemical agents including heavy metals, herbicides, phenols, parthenin, perfluorinated carboxylic

*Corresponding author. E-mail: chris.nweke@futo.edu.ng. Tel: +234(0)8037936150.

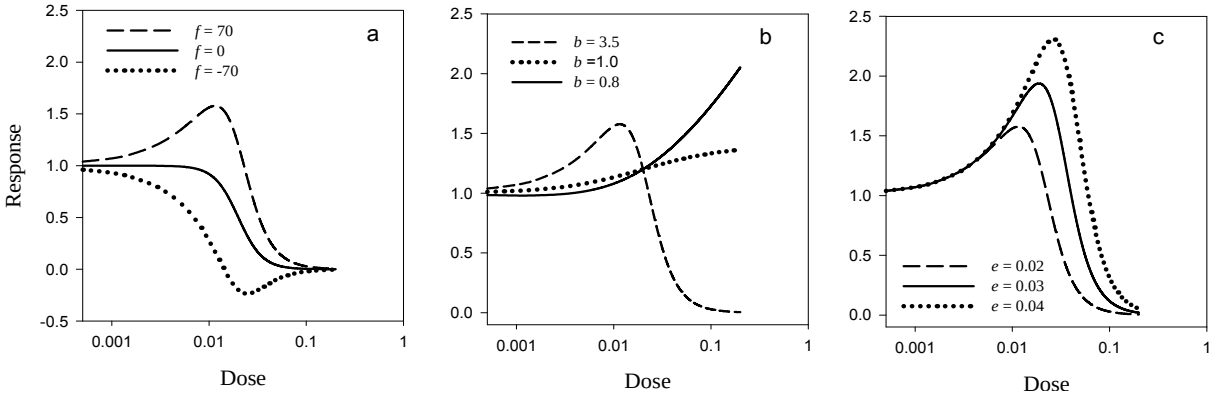

Figure 1. The Brain and Cousens model (Equation 1) with arbitrary values to show effects of *f* parameter (a), *b* parameter (b) and *e* parameter (c) on the curves. The common parameter values are: *c* = 0.0, *d* = 1.0. For a, *b*= 3.5, *e* = 0.02; for b, *f* = 70, *e* = 0.02 and for c, *b* = 3.5, *f* = 70.

acids, antibiotics, mycotoxins, bacteriocins and ionic liquids (Mulkiewicz et al., 2007; Shen et al., 2009; Belz and Cedergreen, 2010; Migliore et al., 2010; Murado and Vázquez, 2010; Belz et al., 2011; Wang et al., 2011; Li et al., 2014; Wang et al., 2014; Nweke et al., 2015). Hormesis has attracted a renewed interest among toxicologists, resulting in the development of new tools to study and accumulate scientific reports on the phenomenon. Thus, there has been a growing interest in statistical models to study hormetic dose-response relationships.

The literature contains a wide range of statistical models for characterizing hormetic dose-response relationships. The applications of these models in toxicological studies with emphasis on their strengths and weaknesses were reviewed by Nweke and Ogbonna (2017). The Brain-Cousens model (Equation 1) derived from the general monotonic log-logistic equation is one of the earliest and well-known dose-response models enabling hormesis (Brain and Cousens, 1989).

$$y = c + \frac{d - c + fx}{1 + \left(\frac{x}{e}\right)^{b}} \quad (1)$$

In Equation 1, *y* is the response, *x* is the dose (concentration), *d* represents the mean response of the untreated control, *c* is the response at infinite dose, *f* measures the rate of stimulation of the response at low dose (*f* > 0 is a necessary condition for the presence of hormesis), *e* and *b* lost their interpretations as the ED_{50} and relative slope at ED_{50}, respectively and thus have no straightforward biological meaning (Schabenberger et al., 1999; Cedergreen et al., 2005). The influences of parameters *f*, *e* and *b* on the shape of the curves are shown in Figure 1. Notably, if the value of *f* is negative, the curve has a valley instead of a peak (Figure 1a).

Although the Brain-Cousens model has been used to describe hormetic dose-response relationships in toxicological studies, it has some drawbacks. The value of *b* in the model is restricted to greater than 1. At *b* < 1 the model does not produce any dose-response curve (Figure 1b) (Cedergreen et al., 2005). Thus, the model cannot describe shallow dose-response curves. The Brain-Cousens model is also less suitable for data exhibiting a broad hormetic dose range and/or an early increase in response at low dose (Belz and Piepho, 2012). In the Brain-Cousens model, the switching function for describing hormesis is linear and curve increases progressively from *d*. Thus, the model cannot describe the initial "no-effect" and pre-stimulation toxicity at low doses (Belz and Piepho, 2012; Beckon et al., 2008). In addition, the Brain-Cousens model has no explicit expression for the ED_{50} and other effective doses. In order to solve this problem, the model was reparameterized to include ED_{50} and other effective doses as parameters in the model (Van Ewijk and Hoekstra, 1993; Schabenberger et al., 1999). The reparameterizations of Brain-Cousens model by Schabenberger et al. (1999) for determination of effective doses (ED_K) and dose of maximum stimulation (*M*) are shown in Equations 2 and 3, respectively.

$$y = c + \frac{d - c + fx}{1 + \left[\frac{K}{100 - K} + \left(\frac{100}{100 - K}\right)\frac{fED_K}{d - c}\right]\left(\frac{x}{ED_K}\right)^{b}} \quad (2)$$

$$y = c + \frac{d - c + fx}{1 + \left(\frac{Mf}{(d - c)b - Mf(1 - b)}\right)\left(\frac{x}{M}\right)^{b}} \quad (3)$$

where K is the percentage inhibition and ED_K is the dose of the effecter that elicited K inhibition of the response (such that K = 50 for ED_{50}, K = -10 for ED_{-10} and K = 0 for *LDS*).

These reparameterized models are used in toxicological studies to estimate the effective doses and their statistical properties (Nweke et al., 2015, 2016; Schabenberger et al., 1999; Zelaya and Owen, 2005; Zou et al., 2013).

Due to the inadequacies of the Brain-Cousens model, Cedergreen et al. (2005) modified the model to introduce a six-parameter version (Equation 4).

$$y = c + \frac{d - c + f\exp\left(-\frac{1}{x^{\alpha}}\right)}{1+\left(\frac{x}{e}\right)^{b}} \quad (4)$$

In Equation 4, *f* is the hormesis parameter (*f* > 0 as a necessary condition for hormesis), parameters *c* and *d* are defined as in Equation 1, while parameters *α*, *b* and *e* have no straightforward biological interpretation (Cedergreen et al., 2005). A reparameterization of Cedergreen-Ritz-Streibig model could be used for estimation of effective doses (ED_K) and dose (*M*) at which maximum stimulation occurred by replacement of parameter *f* with the functions shown in Equations 5 and 6, respectively.

$$f = \frac{\frac{100-\mathrm{K}}{100}(d-c)\left[1+\left(\frac{ED_{\mathrm{K}}}{e}\right)^{b}\right]-(d-c)}{\exp\left(-\frac{1}{ED_{\mathrm{K}}{}^{\alpha}}\right)} \quad (5)$$

$$f = \frac{\left(\frac{M}{e}\right)^{b} b(d-c)}{\exp\left(-\frac{1}{M^{\alpha}}\right)\left[\alpha M^{-\alpha}+\alpha M^{-\alpha}\left(\frac{M}{e}\right)^{b}-\left(\frac{M}{e}\right)^{b} b\right]} \quad (6)$$

According to Cedergreen et al. (2005), the model is more robust in terms of variation of data and describing both very large and relatively small hormetic effects when compared to the Brain-Cousens model. The Cedergreen-Ritz-Streibig model could better describe data sets characterized by early increase in response at low dose and a broad hormetic dose range (Belz and Piepho, 2012). In addition, the model is more flexible than the Brain-Cousens model to describe dose-response relationships where there is toxicity before the initiation of stimulatory response. Belz and Piepho (2012) compared the utility of Brain-Cousens and Cedergreen-Ritz-Streibig models in describing the hormetic response of four plants to fifteen chemical stressors and affirmed that the diverse hormetic dose responses cannot be described by a single model. Some hormetic dose-responses were better described by either Brain-Cousens model or Cedergreen-Ritz-Streibig model. Interestingly, the data set describing the phytotoxic effect of 2-phenylethyl-isothiocyanate on root growth of Amaranthus hybridus could neither be appropriately fitted by the Cedergreen-Ritz-Streibig model nor the Brain-Cousens model (Belz and Piepho, 2012). The improved flexibility of Cedergreen-Ritz-Streibig model was attributed to the introduction of the parameter *α* (Zhu et al., 2013). Nevertheless, the value of *α* has to be fixed when the available data is not enough to determine the rate of increase statistically. In order to allow for explicit determination of effective doses and their statistical properties, Belz and Piepho (2012) reparameterized the original equation. The Cedergreen-Ritz-Streibig model has been widely used to especially describe herbicide hormesis in plants (Cedergreen et al., 2007; 2009; Cedergreen and Olesen, 2010; Belz and Leberle, 2012).

Another model proposed for description of hormetic dose-response relationships is the bilogistic model (Equation 7) of Beckon et al. (2008).

$$y = c + \frac{d - c + \frac{Max - d}{1+\left(\frac{x_1}{x}\right)^{\beta_1}}}{1+\left(\frac{x_2}{x}\right)^{\beta_2}} \quad (7)$$

In Equation 7, parameters *d* and *c* are as defined in Equation 1 and the parameter *Max* is the theoretical maximum (not *ymax*) that would be approached asymptotically by the rising component of the equation in the absence of the descending component (or vice versa), β_1 represents the rising slope (+), x_1 is the dose at midpoint of the rising curve, β_2 represents the falling slope (-), x_2 is the dose at midpoint of the falling curve. The bilogistic model plotted with arbitrary values of the parameters is as shown in Figure 2. The bilogistic model can be viewed as a modification of the Brain-Cousens model, by introduction of a logistic weighting function at hormesis region which describes the rising curve of the dose-response model. The model reduces to log-logistic model if any of the slope parameters is zero, thus allowing simple statistical test for hormesis. The bilogistic model provided better description of hormetic dose-response relationships than the Brain-Cousens model when tested with empirical data (Beckon et al., 2008). The parameter *Max* is only a theoretical maximum and not the actual maximum effect that would be approached by the upslope in the absence of the downslope. Therefore, there is disagreement between the fitted *Max* and its corresponding theoretical interpretation. This limitation has been highlighted by Zhu et al. (2013) and

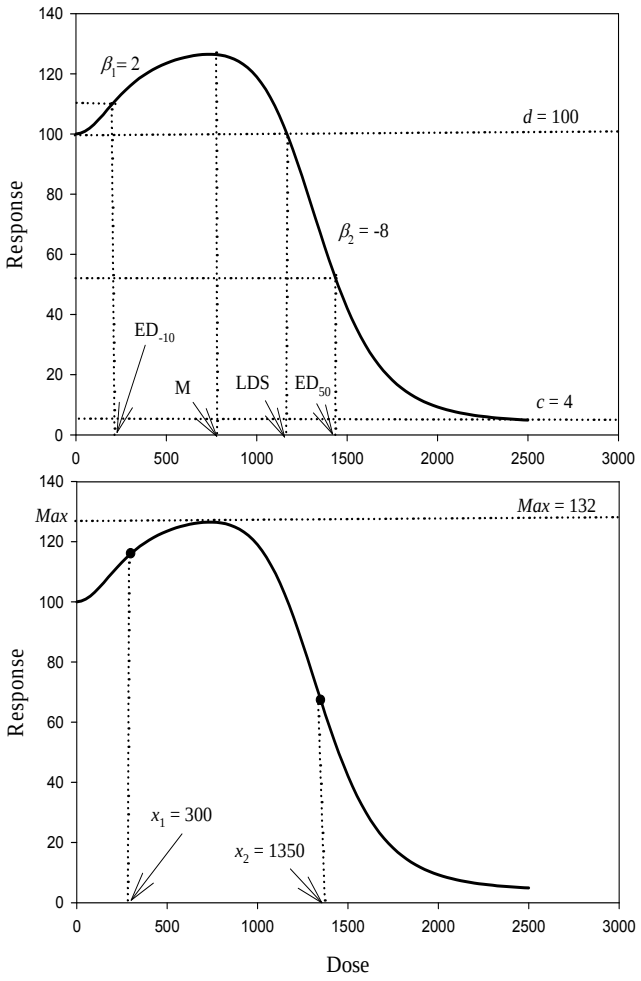

Figure 2. Arbitrary hormesis curve from the bilogistic model of Beckon et al. (2008) for c = 4, d = 100, Max = 132 ($Max \neq$ Maximum y), x_1 = 300, β_1 = 2, x_2= 1350 and β_2 = -8 showing x at maximum response (M), the limiting dose for stimulation (LDS), ED_{-10} and ED_{50} for an inverted U-shaped hormetic dose response curve.

the model was therefore adjudged as inappropriate for describing hormetic data in their study. However, they acknowledged that the bilogistic model is statistically sound and performed better than the Brain-Cousens and Cedergreen-Ritz-Streibig models with respect to the data under review.

The bilogistic model comprises one logistic ascending curve and one logistic descending curve similar to the descending curve of Brain-Cousens and Cedergreen-Ritz-Streibig models. Thus, the model is particularly suited for hormetic data having logistic dose-response relationship at low doses. In addition, the bilogistic model provides considerable improvements when modeling data that include a wide range of doses from well below to well above the dose corresponding to maximum response (Beckon et al., 2008). The bilogistic model, like the original Brain-Cousens and Cedergreen-Ritz-Streibig models, has no explicit parameter for the effective doses. The Brain-Cousens and Cedergreen-Ritz-Streibig models have been extended to allow estimation of effective doses (Van Ewijk and Hoekstra, 1993; Schabenberger et al., 1999; Belz and Piepho, 2012). However, there has been no similar extension of the bilogistic model. According to Zhu et al. (2013), mathematical manipulation is not suitable for the bilogistic model because of its complexity and multiparametric nature. Reparameterization of models for the purpose of estimating effective doses has been discouraged to promote the use of bisection method based on monotone functions (Cedergreen et al., 2005; Zhu et al., 2013). Nonetheless, the computation of effective doses and their standard errors by a combined application of bisection and delta methods has its limitations. Applying the delta method, Cedergreen et al. (2005) could not estimate the limiting dose of stimulation (LDS) which is the dose at which hormesis vanishes (ED_0). In addition, the dose for maximum stimulation (M) was obtained without standard errors and confidence intervals. Thus, use of reparameterized function can be a more convenient tool for estimating effective doses in biphasic dose-responses. Reparameterization of the Cegergreen-Ritz-Sreibig model has been shown to be applicable to calculation of arbitrary effective doses at both stimulatory and inhibitory ranges (Belz and Piepho, 2012, 2015).

A wide range of hormetic dose-response patterns which cannot be described by a particular hormesis model are usually generated in toxicological studies. Each model has its own strengths and weaknesses. Therefore, application of a specific model is dependent on the uniqueness of the data under analysis. The bilogistic model has been shown to be superior to Brain-Cousens and Cedergreen-Ritz-Streibig models in modeling some hormetic dose-responses (Beckon et al., 2008; Belz and Piepho, 2012). Undoubtedly, the model presents an additional statistical tool for the analysis of biphasic dose-response relationships where other models may fail. It is therefore important to reparameterize the model for determination of effective doses and hormesis quantities. This would present expanded possibilities and help to get rid of the bias inherent in using other models for a specific dose-response pattern where the bilogistic model will be more appropriate. Hence, the purpose of the present work was to provide a general method for reparameterization of the bilogistic model to allow for the estimation of effective doses (ED_K) at both stimulatory and inhibitory ranges and the dose at which maximum stimulation occurred (M). Using hormetic dose-responses for illustration, the modeling approach was applied to characterize inverted U-shaped curves.

MATERIALS AND METHODS

Reparameterizations

The bilogistic hormesis model (Beckon et al., 2008) does not

include any effective dose as a parameter in its original form. Thus, this study extended the model to generate other functions that expressed it in terms of parameters that correspond to the effective doses of dose-response relationships. The bilogistic model was reparameterized to incorporate the arbitrary effective doses (ED_K including ED_{-10} [K= -10}, ED_{50} [K= 50] and ED_0 [K = 0] also called LDS) and the dose at which the maximum stimulatory effect occurred (M) by applying the defining relationship described by Schabenberger et al. (1999).

Reparameterization for ED_K

The defining relationship for an arbitrary effective dose (ED_K) for K % inhibition of response is:

$$c + \frac{100 - K}{100} \times (d - c) = c + \frac{(d - c) + \frac{Max - d}{1 + \left(\frac{x_1}{ED_K}\right)^{\beta_1}}}{1 + \left(\frac{x_2}{ED_K}\right)^{\beta_2}} \quad (8)$$

Solving Equation 8 for *Max*, a general expression for ED_K (Equation 9) was obtained, which can be used to determine any arbitrary ED_K by substituting *Max* into Equation 7.

$$Max = \left\{\left[\frac{100 - K}{100} \times (d - c) \times \left[1 + \left(\frac{x_2}{ED_K}\right)^{\beta_2}\right] - (d - c)\right] \times \left[1 + \left(\frac{x_1}{ED_K}\right)^{\beta_1}\right]\right\} + d \quad (9)$$

Rewriting Equation 9 for ED_{-10} (K = -10 representing the concentration that elicited 10% stimulation and -10% inhibition. In inverted U-shaped curves, it is also the value of x at y =110% of control), *LDS* (K = 0) and ED_{50} (K = 50), Equations 10, 11 and 12, respectively were obtained.

$$Max = \left\{\left[(d - c)\left(0.1 + 1.1\left(\frac{x_2}{ED_{-10}}\right)^{\beta_2}\right)\right] \times \left[1 + \left(\frac{x_1}{ED_{-10}}\right)^{\beta_1}\right]\right\} + d \quad (10)$$

$$Max = \left\{(d - c) \times \left(\frac{x_2}{LDS}\right)^{\beta_2} \times \left[1 + \left(\frac{x_1}{LDS}\right)^{\beta_1}\right]\right\} + d \quad (11)$$

$$Max = \left\{0.5 \times (d - c) \times \left[\left(\frac{x_2}{ED_{50}}\right)^{\beta_2} - 1\right] \times \left[1 + \left(\frac{x_1}{ED_{50}}\right)^{\beta_1}\right]\right\} + d \quad (12)$$

Substituting *Max* (in Equations 10 to 12) into the original bilogistic model (Equation 7), leads to extended functions allowing for hormesis and in which ED_{-10}, *LDS*, and ED_{50} can be incorporated.

Reparameterization for M

In order to obtain the expression for the dose M, at which maximum stimulatory effect occurred, Equation 7 was differentiated with respect to x to obtain the first derivative of the function. In order to achieve this, Equation 7 was first simplified as Equation 13 and differentiated with respect to x.

$$y = \frac{c\left(\frac{x_2}{x}\right)^{\beta_2} + c\left(\frac{x_1}{x}\right)^{\beta_1}\left(\frac{x_2}{x}\right)^{\beta_2} + d\left(\frac{x_1}{x}\right)^{\beta_1} + Max}{1 + \left(\frac{x_1}{x}\right)^{\beta_1} + \left(\frac{x_2}{x}\right)^{\beta_2} + \left(\frac{x_1}{x}\right)^{\beta_1}\left(\frac{x_2}{x}\right)^{\beta_2}} \quad (13)$$

$$\frac{dy(x)}{dx} = 0 =$$
$$\left\{\left[c\left(\frac{x_2}{M}\right)^{\beta_2} + c\left(\frac{x_1}{M}\right)^{\beta_1}\left(\frac{x_2}{M}\right)^{\beta_2} + d\left(\frac{x_1}{M}\right)^{\beta_1} + Max\right] \times \left[x_1{}^{\beta_1}\beta_1 M^{-\beta_1 - 1} + x_2{}^{\beta_2}\beta_2 M^{-\beta_2 - 1} + x_1{}^{\beta_1}x_2{}^{\beta_2}(\beta_1 + \beta_2) M^{-\beta_1 - \beta_2 - 1}\right]\right\}$$
$$- \left\{\left[1 + \left(\frac{x_1}{M}\right)^{\beta_1} + \left(\frac{x_2}{M}\right)^{\beta_2} + \left(\frac{x_1}{M}\right)^{\beta_1}\left(\frac{x_2}{M}\right)^{\beta_2}\right] \times \left[cx_2{}^{\beta_2}\beta_2 M^{-\beta_2 - 1} + cx_1{}^{\beta_1}x_2{}^{\beta_2}(\beta_1 + \beta_2) M^{-\beta_1 - \beta_2 - 1} + dx_1{}^{\beta_1}\beta_1 M^{-\beta_1 - 1}\right]\right\} \quad (14)$$

$$Max = \frac{(f_1 \times f_2) - (f_3 \times f_4)}{f_4} \quad (15)$$

where

$$f_1 = \left[1 + \left(\frac{x_1}{M}\right)^{\beta_1} + \left(\frac{x_2}{M}\right)^{\beta_2} + \left(\frac{x_1}{M}\right)^{\beta_1}\left(\frac{x_2}{M}\right)^{\beta_2}\right]$$

$$f_2 = \left[c x_2{}^{\beta_2}\beta_2 M^{-\beta_2 - 1} + c x_1{}^{\beta_1}x_2{}^{\beta_2}(\beta_1 + \beta_2) M^{-\beta_1 - \beta_2 - 1} + d x_1{}^{\beta_1}\beta_1 M^{-\beta_1 - 1}\right]$$

$$f_3 = \left[c\left(\frac{x_2}{M}\right)^{\beta_2} + c\left(\frac{x_1}{M}\right)^{\beta_1}\left(\frac{x_2}{M}\right)^{\beta_2} + d\left(\frac{x_1}{M}\right)^{\beta_1}\right]$$

$$f_4 = \left[x_1{}^{\beta_1}\beta_1 M^{-\beta_1 - 1} + x_2{}^{\beta_2}\beta_2 M^{-\beta_2 - 1} + x_1{}^{\beta_1}x_2{}^{\beta_2}(\beta_1 + \beta_2) M^{-\beta_1 - \beta_2 - 1}\right]$$

Table 1. Syntax for reparameterization of Beckon et al. (2008) model for estimation of arbitrary effective doses.

Effective doses	Parameter to be replaced[a]	Model expression y[*x*]= *c*+(((*d*-*c*)+((*Max*-*d*)/(1+((*x*$_1$/*x*)^β_1))))/(1+((*x*$_2$/*x*)^β_2)))
ED$_{-10}$	*max* =	(((*d*-c)*(0.1+(1.1*((*x*$_2$/*ED*$_{-10}$)^β_2))))*(1+((*x*$_1$/*ED*$_{-10}$)^β_1)))+*d*
LDS	*max* =	((*d*-*c*)*((*x*$_2$/*LDS*)^β_2)*(1+((*x*$_1$/*LDS*)^β_1)))+*d*
ED$_{50}$	*max* =	(0.5*(*d*-*c*)*(((*x*$_2$/*ED*$_{50}$)^β_2)-1)*(1+((*x*$_1$/*ED*$_{50}$)^β_1)))+*d*
M	*max* =	(((1+((*x*$_1$/*M*)^β_1)+((*x*$_2$/*M*)^β_2)+((*x*$_1$/*M*)^β_1)*((*x*$_2$/*M*)^β_2))*((*c**(*x*$_2$^β_2)*β_2*(*M*^(-β_2-1)))+(*c**(*x*$_1$^β_1)*(*x*$_2$^ β_2)*(β_1+β_2)*(*M*^(-β_1-β_2-1)))+(*d**(*x*$_1$^β_1)*(*M*^(-β_1-1)))))- (((*c**((*x*$_2$/*M*)^β$_2$))+(*c**((*x*$_1$/*M*)^β_1)*((*x*$_2$/*M*)^β_2))+(*d**((*x*$_1$/*M*)^β_1)))*(((*x*$_1$^β_1)*β_1*(*M*^(-β_1-1)))+((*x*$_2$^β_2)* β_2*(*M*^(-β_2-1)))+((*x*$_1$^β_1)*(*x*$_2$^β_2)*(β_1+β_2)*(*M*^(-β_1- β_2-1))))))/(((*x*$_1$^β_1)*β_1*(*M*^(-β_1-1)))+((*x*$_2$^β_2)* β_2*(*M*^(-β_2-1)))+((*x*$_1$^β_1)*(*x*$_2$^β_2)*(β_1+β_2)*(*M*^(-β_1- β_2-1))))

[a]Parameter *max* to be replaced in the model expression, *LDS* = limited dose for stimulation, *ED*$_{50}$ = effective dose (50%), *ED*$_{-10}$ = effective dose (-10%); *M* = maximum stimulatory dose.

The first derivative of the function must equal zero at maximum stimulation (*x*=*M*). Thus, the defining relationship as shown in Equation 14 was obtained. Solving Equation 14 for *Max* gives Equation 15. By substituting *Max* (in Equation 15) into Equation 7, a 7-parameter hormesis dose-response model for the incorporation of *M* into the bilogistic model was obtained. Although these models appear complex, they can easily be coded into a nonlinear regression package using syntaxes shown in Table 1.

The hormesis data

Three sets of hormetic dose-response data from three different experimental systems were used in this study to evaluate the original and the reparameterized models. The dose-response data include: (1) the biphasic effects of penicillin on growth of *Staphylococcus* species (Beckon et al., 2008). The growth of *Staphylococcus* sp. at different concentrations of penicillin was transformed relative to the control response (% of control) as described by Nweke and Ogbonna (2017), (2) the biphasic effects of 1-hexyl-3-methyl-imidazolium chloride ([HMIM]Cl) on firefly luciferase activity after 15-min exposure (Zhu et al., 2013). The relative luminescence units (RLUs) of the luciferase exposed to [HMIM]Cl were measured with SpectraMax M5 microplate reader (Molecular Devices Inc., USA) with a 96-well microplate (Zhu et al., 2013). The data were transformed to percent inhibition by multiplying the relative ratios by 100 and then converted to an inverted U-shaped dose-response relationship (% of control) by subtracting the percent inhibition from 100 as described elsewhere (Nweke and Ogbonna, 2017) and (3) the biphasic effects of 4-chlorophenol (4-CP) on *Providencia vermicola* dehydrogenase activity. The assay was based on reduction of 2,3,5-triphenyltetrazolium chloride to triphenyl formazan in response to varying concentrations of 4-CP. The data were generated in our laboratory using 24-h dehydrogenase activity assay as described by Nweke et al. (2014). The concentration-effect data were transformed relative to control as described by Nweke and Ogbonna (2017).

Dose-response modeling

As mentioned earlier, the Beckon et al. (2008) model (Equation 7) reduces to log-logistic model if any of the slope parameters (β_1 and β_2) is zero, thus allowing simple statistical test for hormesis. The growth of *Staphylococcus* sp., firefly luciferase activity or dehydrogenase activity in *P. vermicola* as a function of concentrations of penicillin, [HMIM]Cl or 4-CP respectively were fitted into the original model (Equation 7) using user-defined function in TableCurve 2D v. 5.01 curve fitting software by least squares minimization of residuals to test for the statistical significance of hormesis. In all data, the 95% confidence interval of the slopes β_1 and β_2 did not include zero indicating significant hormetic effects of the respective substance on the tested response. The parameters of the model were estimated freely without constraint at the first instance. The data were also fitted to Equation 7 without constraint on *c* while *d* was fixed at 100% and then with *c* and *d* fixed at 0 and 100%, respectively. The initial values of x_1, x_2, *c* and *d* used in the curve fitting were graphically deduced from *x*-*y* data plots. The initial values of *Max*, β_1 and β_2 were manually adjusted until the predicted curve became close to the observed data. Subsequently, all parameters were automatically optimized to best initial parameter estimates in TableCurve 2D software. The values of *ED*$_{-10}$, *LDS*, *ED*$_{50}$ and *M* were estimated by reparameterization according to Equations 10, 11, 12 and 15, respectively using graphically-anticipated initial parameters as optimized in TableCurve 2D. The *ED*$_{-10}$ has two possible values, one on the left side of *M* (*ED*$_{-10L}$) and another on the right side of *M* (*ED*$_{-10R}$). In order to differentiate the two *ED*$_{-10}$ values, constraint was applied to limit value below or above *M*. The model parameters were estimated with *d* fixed at 100% and with *c* and *d* fixed at 0 and 100%, respectively while fitting *ED*$_{-10}$, *LDS*, *ED*$_{50}$ and *M* reparameterizations. The value of y_{max} was computed from the mean value of *M* and other parameters by using the *M* reparameterization.

In order to compare the bilogistic model of Beckon et al. (2008) with Brain-Cousens and Cedergreen-Ritz-Streibig models, the hormesis data were also fitted with the two models in their original forms using TableCurve 2D as described earlier. Models were compared based on three goodness-of-fit statistics: Adjusted coefficient of determination (R^2adj), root mean squared error (RMSE) and Akaike information criterion (AIC). The calculation of R^2adj was implemented in TableCurve 2D V5.01. The RMSE was calculated as shown in Equation 16.

$$\mathrm{RMSE} = \sqrt{\frac{\sum \mathrm{Residual}^2}{n-m}} \tag{16}$$

where residual is the difference between the observed and predicted responses, *n* is the number of observations and *m* is the number of model parameters.

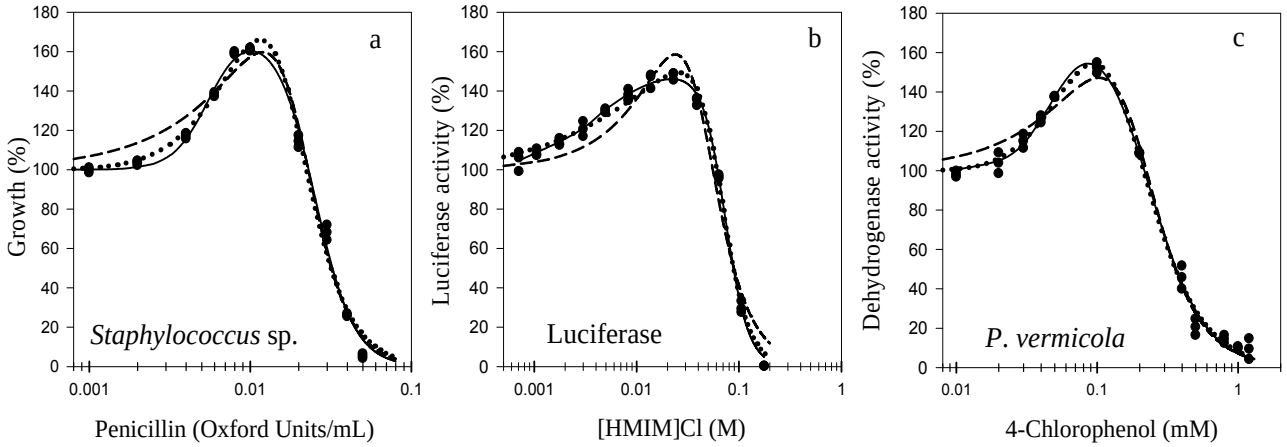

Figure 3. Observed (data points) and predicted (lines) effects of: (a) penicillin on the growth of *Staphylococcus* species (Beckon et al., 2008), (b) 1-hexyl-3-methyl-imidazolium chloride [HMIM]Cl on firefly luciferase activity (Zhu et al., 2013), and (c) 4-chlorophenol on *P. vermicola* dehydrogenase activity. Predictions were according to the Brain and Cousens (1989) model (Equation 1) [dashed line], Cedergreen et al. (2005) model (Equation 4) [dotted line] and Beckon et al. (2008) model (Equation 7) [solid line]. Parameters *c* and *d* were fixed at 0 and 100, respectively.

The AIC values were generated by performing nonlinear regression in SAS 9.2 statistical software. In addition, the effective doses and the dose at maximum stimulation (*M*) for all the dose-response relationships were also calculated by fitting the data into the reparameterized Brain-Cousens (Equations 2 and 3) and Cedergreen-Ritz-Streibig (Equations 5 and 6 substituted into Equation 4) models. The values obtained from the three models were compared using Duncan post-hoc tests implemented with IBM SPSS Statistics 25.

RESULTS

Figure 3 shows the three data sets as observed responses as well as responses predicted from the original Brain-Cousens (Equation 1), Cedergreen-Ritz-Streibig (Equation 4) and bilogistic (Equation 7) models. All the three hormesis data sets were well fitted by each of the three models and detected significant hormetic effects of penicillin, 1-hexyl-3-methyl-imidazolium chloride and 4-CP on the growth of *Staphylococcus* sp., firefly luciferase activity and dehydrogenase activity in *P. vermicola*, respectively. The Brain-Cousens and Cedergreen-Ritz-Streibig models can be reduced to monotonic sigmoidal model if *f* equals zero. The values of *f* ($p < 0.01$) in both models for all the data sets did not include zero. In all the data sets, 95% confidence interval of the slopes and the p values ($p < 0.01$) showed that β_1 and β_2 did not include zero indicating significant hormetic effects of the respective substance (Table 2). The Brain-Cousens model could fit the data sets fairly well with the lowest adjusted R^2 which were greater than 0.97(penicillin data), 0.95 ([HMIM]Cl data) and 0.98 (4-CP data). The bilogistic model of Beckon et al. (2008) had the lowest RMSE for all the data sets (Figure 4). With the exception of 4-CP data set, the bilogistic model had the lowest AIC values in all the data sets. Judging from the plots and residuals, the bilogistic model provided a better description of the three hormesis data especially at low doses. At high doses, described by the downward curve ($x \geq$ M), the responses predicted from the three model tend to overlap indicating insignificant differences between them (Figure 3). Generally, the order of goodness-of-fit of the bilogistic model for the hormesis data was, effects of ionic liquid on luciferase activity > effects of 4-chlorophenol on *P. vermicola* dehydrogenase activity > effects of penicillin on the growth of *Staphylococcus* sp.

The parameters and their statistical properties as derived from the original model are shown in Table 2. Applying constraint on parameters *c* and *d* has bearing upon the estimated values of other parameters. In *Staphylococcus* sp. and luciferase data sets, the estimated value of *Max* increased when *d* was fixed at 100% and *c* allowed to be determined iteratively (Table 2). In addition, this reduced the values of β_1, increased the value of β_2 and increased the value of x_1. Conversely, in the *P. vermicola* data, fixing *d* at 100% and allowing *c* to be determined iteratively reduced the value of *Max*, increased the value of β_1, reduced the value of β_2 and reduced the value of x_1. Generally, allowing *c* to be determined resulted to a better goodness-of-fit in terms of the R^2. However, unrealistic negative values of *c* were produced in *Staphylococcus* and luciferase data sets. In *P. vermicola* data set, positive value of *c* was determined. This is because the response did not tend to zero with increasing concentrations of 4-CP.

The model parameters and their statistical properties derived from the ED_{-10}, *LDS*, ED_{50} and *M* reparameterizations are shown in Tables 3 to 5. Generally, allowing *c* to be determined improved the

Table 2. Model parameters and their statistical properties derived from original Beckon et al. (2008) model.

Parameter	Data sets[a]		
	Staphylococcus species[†]	Luciferase[‡]	*Providencia vermicola*
c= 0			
c (%) fixed	0	0	0
d (%)	101.355 ± 2.293** (96.622 – 106.089)	102.697 ± 3.187** (96.187 – 109.206)	95.663 ± 4.104** (87.281 – 104.046)
Max (%)	171.341 ± 8.054** (154.719 – 187.963)	150.266 ± 3.137** (143.859 – 156.674)	213.691 ± 53.974* (103.461 – 323.921)
x_1	0.0056 ± 0.0004 (U/mL)** (0.0004 – 0.006)	0.0040 ± 0.0005 (M)** (0.003 – 0.005)	0.0596 ± 0.0196 (mM)* (0.020 – 0.100)
β_1	4.212 ± 0.985 (%mL/U)* (2.178 – 6.246)	1.586 ± 0.353 (%/M)** (0.864 – 2.308)	2.217 ± 0.671 (%/mM)* (0.847 – 3.587)
x_2	0.0253 ± 0.0009 (U/mL)** (0.023 – 0.027)	0.074 ± 0.001 (M)** (0.071 – 0.076)	0.2087 ± 0.0408 (mM)** (0.125 – 0.292)
β_2	-3.591 ± 0.245 (%mL/U)** (-4.097 – -3.086)	-3.901 ± 0.177 (%/M)** (-4.263 – -3.539)	-2.118 ± 0.182 (%/mM)** (-2.489 – -1.747)
R^2 (R^2 adj)	0.9916 (0.9894)	0.9959 (0.9950)	0.9937 (0.9924)
d =100			
c (%)	-66.978 ± 31.621* (-132.240 – -1.716)	-9.379 ± 2.806* (-15.111 – -3.647)	6.648 ± 2.100* (2.360 – 10.937)
d (%) fixed	100	100	100
Max (%)	221.999 ± 52.565** (113.511 – 330.486)	155.777 ± 3.660** (148.303 – 163.251)	169.286 ± 8.664** (151.591– 186.981)
x_1	0.0065 ± 0.0008 (U/mL)** (0.005 – 0.008)	0.0044 ± 0.0006 (M)** (0.003 – 0.006)	0.0457 ± 0.0039 (mM)** (0.038 – 0.054)
β_1	3.154 ± 0.595 (%mL/U)** (1.926 – 4.382)	1.272 ± 0.127 (%/M)** (1.012 – 1.532)	3.223 ± 0.533 (%/mM)** 2.134 – 4.312
x_2	0.0274 ± 0.0028 (U/mL)** (0.022 – 0.033)	0.0758 ± 0.0013 (M)** (0.073 – 0.079)	0.2456 ± 0.0119 (mM)** 0.221 – 0.270
β_2	-1.848 ± 0.527 (%mL/U)* (-2.936 – -0.761)	-3.333 ± 0.186 (%/M)** (-3.714 – -2.953)	-2.731 ± 0.232 (%/mM)** -3.205 – -2.257
R^2 (R^2 adj)	0.9977(0.9971)	0.9972 (0.9966)	0.9948 (0.9937)
c = 0, d = 100			
c (%) fixed	0	0	0
d (%) fixed	100	100	100
Max (%)	172.375 ± 8.358** (155.161 – 189.588)	151.722 ± 2.913** (145.780 – 157.663)	188.967 ± 18.210** (151. 828 –226.106)
x_1	0.0055 ± 0.0004 (U/mL)** (0.005 – 0.006)	0.0038 ± 0.0005 (M)** (0.003 – 0.005)	0.0517 ± 0.0068 (mM)** (0.038 – 0.066)
β_1	3.971 ± 0.822 (%mL/U)** (2.278 – 5.664)	1.375 ± 0.155 (%/M)** (1.059 – 1.691)	2.881 ± 0.514 (%/mM)** (1.832 – 3.931)
x_2	0.0252 ± 0.0009 (U/mL)** (0.023 – 0.027)	0.0734 ± 0.0011 (M)** (0.071 – 0.076)	0.2295 ± 0.0220 (mM)** (0.185 – 0.274)
β_2	-3.575 ± 0.242 (%mL/U)** (-4.074 – -3.077)	-3.870 ± 0.169 (%/M)** (-4.215 – -3.525)	-2.199 ± 0.158 (%/mM)** (-2.521 – -1.878)
R^2 (R^2 adj)	0.9915 (0.9897)	0.9958 (0.9951)	0.9934 (0.9923)

[a]Data are given as mean ± standard error with 95% confidence interval in parentheses. [†]Data from Beckon et al. (2008). [‡]Data from Zhu et al. (2013). **P < 0.0001for the estimated parameters. *P < 0.01for the estimated parameters

goodness-of-fit characteristics in all the data sets. The reparameterization of the bilogistic model did not affect the goodness-of-fit characteristics. The values of the adjusted R^2 remained same with all reparameterizations for a particular hormesis data. In addition, reparameterization of the model for a particular effective dose did not affect estimation of other parameters (such as x_1, x_2, β_1, $\beta_2$and M). In each hormesis data, the values of each parameter either remained same or varied insignificantly ($p > 0.05$) in different model reparameterizations.

The goodness-of-fit statistics for the hormesis data fitted to the hormesis models in their original forms are as shown in Figure 4. The comparison of effective doses derived from the three hormesis models for the three data sets are shown in Table 6. The ED_{50} of penicillin, 1-hexyl-3-methyl-imidazolium chloride and 4-CP derived from the bilogistic model were 0.032 ± 0.001 U/ml, 0.088 ± 0.001 M and 0.365 ± 0.008 mM, respectively. The dose of maximum stimulation (M) obtained from the bilogistic model were 0.0101 ± 0.0005 U/ml, 0.0221 ± 0.0009 M and 0.086 ± 0.004 mM for penicillin, 1-hexyl-3-methyl-imidazolium chloride and 4-CP, respectively. There were no significant differences among the ED_{50} and M values derived from the three models for all the hormetic dose-response relationships. With the exception of the luciferase data, the LDS values of penicillin and 4-CP did not vary significantly among the three hormesis models. Generally, the ED_{-10L} obtained from Brain-Cousens model differed significantly from the values obtained from the other models. The Brain-Cousens and Cedergreen-Ritz-Streibig models overestimated the y_{max} in the penicillin and 1-hexyl-3-methyl-imidazolium chloride data. In the 4-CP data, the Brain-Cousens model underestimated underestimated the *ymax*.

Table 3. Parameters derived from reparameterized models based on the effects of penicillin on *Staphylococcus* species growth.

Parameter[a]	Bilogistic model (Equation 7) reparameterized for incorporation of:			
	ED_{-10L}	*LDS*	ED_{50}	*M*
d = 100				
c (%)	-66.762 ± 31.464* (-131.700 – -1.824)	-66.094 ± 30.984* (-130.042– -2.145)	-66.230 ± 31.095* (-130.407– -2.052)	-66.760 ± 31.510* (-131.793– -1.726)
d (%) fixed	100	100	100	100
x_1 (U/mL)	0.0065 ± 0.0008** (0.0048 – 0.0082)	0.0065 ± 0.0008** (0.0049 – 0.0081)	0.0065 ± 0.0008*** (0.0049 – .0082)	0.0065 ± 0.0008** (0.0048 – 0.0082)
β_1 (%mL/U)	3.158 ± 0.593** (1.935 – 4.381)	3.169 ± 0.585** (1.962 – 4.376)	3.165 ± 0.587** (1.953 – 4.377)	3.154 ± 0.593** (1.929 – 4.379)
x_2 (U/mL)	0.027 ± 0.003** (0.021 – 0.033)	0.027 ± 0.003** (0.022 – 0.033)	0.027 ± 0.003** (0.022 – 0.033)	0.027 ± 0.003** (0.022 – 0.033)
β_2 (%ml/U)	-1.852 ± 0.525* (-2.936 – -0.768)	-1.864 ± 0.520* (-2.937 – -0.790)	-1.860 ± 0.522* (-2.938 – -0.783)	-1.851 ± 0.527* (-2.938 – -0.764)
ED_{-10L} (U/mL)	0.0040 ± 0.0003** (0.0035 – 0.0046)	-	-	-
LDS (U/mL)	-	0.023 ± 0.0002** (0.022 – 0.023)	-	-
ED_{50} (U/mL)	-	-	0.044 ± 0.006** (0.031 – 0.058)	-
M (U/mL)	-	-	-	0.0099 ± 0.0003** (0.0093 – 0.0105)
ymax (%)	-	-	-	165.140
R^2 (R^2 adj)	0.998 (0.997)	0.998 (0.997)	0.998 (0.997)	0.998 (0.997)
c= 0, *d* = 100*				
c (%) fixed	0	0	0	0
d (%) fixed	100	100	100	100
x_1 (U/mL)	0.0055 ± 0.0004** (0.0046 – 0.0064)	0.0055 ± 0.0004** (0.0046 – 0.0064)	0.0055 ± 0.0004** (0.0046 – 0.0064)	0.0055 ± 0.0004** (0.0046 – 0.0064)
β_1 (%mL/U)	3.971 ± 0.822** (2.278 – 5.664)	3.971 ± 0.822** (2.278 – 5.664)	3.971 ± 0.822** (2.278 – 5.664)	3.971 ± 0.822** (2.278 – 5.664)
x_2 (U/mL)	0.0252 ± 0.0009** (0.0233 – 0.0270)	0.0252 ± 0.0009** (0.0233 – 0.0270)	0.0252 ± 0.0009** (0.0233 – 0.0270)	0..0252 ± 0.0008** (0.0233 – 0.0270)
β_2 (%mL/U)	-3.575 ± 0.242** (-4.074 – -3.077)	-3.575 ± 0.242** (-4.074 – -3.077)	-3.575 ± 0.242** (-4.074 – -3.077)	-3.575 ± 0.242** (-4.074 – -3.077)
ED_{-10L} (U/mL)	0.0035 ± 0.0003** (0.0029 – 0.0040)	-	-	-
LDS (U/mL)	-	0.0230 ± 0.0004** (0.0222 – 0.0238)	-	-
ED_{50} (U/mL)	-	-	0.0323 ± 0.0005** (0.0313 – 0.3334)	-
M (U/mL)	-	-	-	0.0101 ± 0.0005** (0.0090 – 0.0112)
ymax (%)	-	-	-	161.038
R^2 (R^2 adj)	0.991 (0.990)	0.991 (0.990)	0.991 (0.990)	0.991 (0.990)

[a]Data are given as mean ± standard error with 95% confidence interval in parentheses ,**P < 0.0001for all estimated parameters; *P < 0.01 for the estimated parameters.

DISCUSSION

Modeling biphasic dose-response relationship is important for optimizing plant, animal and human nutrition and for accurate evaluation of the effectiveness and toxicity of pharmaceuticals and other chemicals that produce biphasic effects (Beckon et al., 2008). Accurate descriptions of hormetic dose-response relationship have bearing upon establishment of safe limits for hormetic substances including food additives, drugs and environmental pollutants. Mathematical models are important tool for understanding the biological bases of dose-response relationship leading to improvements in protection of plant, animal, human and environmental health. In this case, the bilogistic model proposed by Beckon et al. (2008) presented a formidable tool to characterize effects of substances that produce both stimulatory and inhibitory effects on living system. The bilogistic model was shown to be superior to Brain-Cousens and Cedergreen-Ritz-Streibig models in describing the three hormetic data sets presented in this study. According to the goodness-of-fit statistics (R^2, RMSE and AIC), the bilogistic model of Beckon et al. (2008) provided a better description of the hormesis data. Generally, the graphical agreement between observed and fitted values in all the hormesis data was best with the bilogistic model. Although the Cedergreen- Ritz-Streibig model produced somehow similar results when compared with the bilogistic model, it overestimated the value of y_{max} in the *Staphylococcus* data set. The major difference observed in the fitting of the data to the models occurred mainly at low dose region. The ED_{-10L} values for instance obtained from the Brain-Cousens model for all the hormesis data are significantly lower or higher than values obtained from the other models. The high dose region (x ≥ M) described by the downward curve seems to be unaffected. This could be attributed to the fact that in all the models, the switching function that determines the downward curve is same logistic function. The switching function describing the low doses is linear for Brain-Cousens model but logistic for the bilogistic model. Thus, the Beckon et al. (2008) model would be particularly suited for data with logistic dose-response relationship at low doses ($0 \leq x \leq M$) to be described by

Table 4. Parameters derived from reparameterized models based on the effects of 1-hexyl-3-methyl-imidazolium chloride [HMIM]Cl on firefly luciferase activity.

Parameter	Bilogistic model (Equation 7) reparameterized for incorporation of:			
	ED_{-10L}	LDS	ED_{50}	M
d = 100				
c (%)	-9.379 ± .2.807* (-15.111 – -3.647)	-9.379 ± 2.807* -15.111 – -3.647)	-9.379 ± 2.807* (-15.111 – -3.647)	-9.379 ± 2.807* (-15.111 – -3.647)
d (%) fixed	100	100	100	100
x_1 (M)	0.0044 ± 0.0006** (0.0032 – 0.0056)	0.0044 ± 0.0006** (0.0032 – 0.0056)	0.0044 ± 0.0006** (0.0032 – 0.0056)	0.0044 ± 0.0006** (0.0032 – 0.0056)
β_1 (%/M)	1.272 ± 0.127** (1.012 – 1.532)	1.272 ± 0.127** (1.012 – 1.532)	1.272 ± 0.127** (1.012 – 1.532)	1.272 ± 0.127** (1.012 – 1.532)
x_2 (M)	0.076 ± 0.001** (0.073 – 0.079)	0.076 ± 0.001** (0.073 – 0.079)	0.076 ± 0.001** (0.073 – 0.079)	0.076 ± 0.001** (0.073 – 0.079)
β_2 (%/M)	-3. 333 ± 0.186** (-3.714 – -2.953)	-3. 333 ± 0.186** (-3.714 – -2.953)	-3.333 ± 0.186** (-3.714 – -2.953)	-3.333 ± 0.186** (-3.714 – -2.953)
ED_{-10L} (M)	0.0015 ± 0.0001** 0.0012 – 0.0017)	-	-	-
LDS (M)	-	0.0613 ± 0.0007** (0.0599 – 0.0627)	-	-
ED_{50} (M)	-	-	0.093 ± 0.002** (0.090 – 0.097)	-
M (M)	-	-	-	0.0212 ± 0.0008** (0.0196 – 0.0228)
$ymax$ (%)	-	-	-	146.368
R^2 (R^2 adj)	0.9972 (0.9966)	0.9972 (0.9966)	0.9972 (0.9966)	0.9972 (0.9966)
c = 0, d = 100				
c (%) fixed	0	0	0	0
d (%) fixed	100	100	100	100
x_1 (M)	0.0038 ± 0.0005** (0.0029 – 0.0048)	0.0038 ± 0.0005** (0.0029 – 0.0048)	0.0038 ± 0.000** (0.0029 – 0.0048)	0.0038 ± 0.0005** (0.0029 – 0.0048)
β_1 (%/M)	1.375 ± 0.155** (1.059 – 1.691)	1.375 ± 0.155** (1.059 – 1.691)	1.375 ± 0.155** (1.059 – 1.691)	1.375 ± 0.155** (1.059 – 1.691)
x_2 (M)	0.073 ± 0.001** (0.071 – 0.076)	0.073 ± 0.001** (0.071 – 0.076)	0.073 ± 0.001** (0.071 – 0.076)	0.073 ± 0.001** (0.071 – 0.076)
β_2 (%/M)	-3. 870 ± 0.169** (-4.215 – -3.525)	-3. 870 ± 0.169** (-4.215 – -3.525)	-3. 870 ± 0.169** (-4.215 – -3.525)	-3. 870 ± 0.169** (-4.215 – -3.525)
ED_{-10L} (M)	0.0014 ± 0.0001** 0.0011– 0.0016)	-	-	-
LDS (M)	-	0.0616 ± 0.0008** (0.0600 – 0.0632)	-	-
ED_{50} (M)	-	-	0.0881 ± 0.0011** (0.0858 – 0.0903)	-
M (M)	-	-	-	0.0221 ± 0.0009** (0.0200 – 0.0241)
$ymax$ (%)				148.944
R^2 (R^2 adj)	0.9958 (0.9951)	0.9958 (0.9951)	0.9958 (0.9951)	0.9958 (0.9951)

[a]Data are given as mean ± standard error with 95% confidence interval in parentheses. **P < 0.0001for all estimated parameters. *P < 0.01for the estimated parameters.

upward curve. A typical example is hormetic data having delayed stimulation at low doses. In addition, Beckon et al. (2008) model can represent dose-responses across a wide range of doses. In toxicological studies, a wide variety of dose-response patterns are generated which cannot all be described by any known single model. The bilogistic model is therefore an important candidate in the list of models for description of hormetic dose response relationships.

Given that hormesis is becoming more frequent in toxicological studies and that the bilogistic model describes certain hormetic dose-response relationship better than other models, it is necessary to describe a method for determination of effective doses using this model. The application of the bilogistic model when it offers better fit to a dose-response data will help to get rid of errors inherent in using other models that do not adequately describe a hormetic data or in ignoring response stimulation at sub-inhibitory doses. According to Schabenberger et al. (1999), ignoring hormesis and fitting data with monotonic function can lead to substantial bias in estimates of effective dosages. Although Zhu et al. (2013) suggested that mathematical manipulation is not suitable for a complex expression like the bilogistic model of Beckon et al. (2008), this study successfully extended the bilogistic model to enable estimation of any effective dose while accommodating hormesis. The extensions presented here allows determination of effective doses at both stimulatory and inhibitory dose ranges.

Fitting data to nonlinear model with many parameters such as the bilogistic model can potentially be challenging. There is no explicit expression for the parameters of this model and so the parameter values must be estimated by iterative process. The ability of nonlinear regression to achieve rapid convergence partly depends on good initial parameter estimates (Mcmeekin et al., 1999). Selecting good initial estimates of the model

Table 5. Parameters derived from original and reparameterized models based on the effects of 4-chlorophenol on *P. vermicola* dehydrogenase activity.

Parameter	Bilogistic model (Equation 7) reparameterized for incorporation of:			
	ED_{-10L}	*LDS*	ED_{50}	*M*
d = 100				
c (%)	6.648 ± 2.100* (2.360 –10.937)	6.648 ± 2.100* (2.360 – 10.937)	6.648 ± 2.100* (2.360 – 10.937)	6.648 ± 2.100* (2.360 – 10.937)
d (%) fixed	100	100	100	100
x_1 (mM)	0.046 ± 0.004** (0.038 – 0.054)	0.046 ± 0.004** (0.038 – 0.054)	0.046 ± 0.004** (0.038 – 0.054)	0.046 ± 0.004** (0.038 – 0.054)
β_1 (%/mM)	3.223 ± 0.533** (2.134 – 4.312)	3.223 ± 0.533** (2.134 – 4.312)	3.223 ± 0.533** (2.134 – 4.312)	3.223 ± 0.533** (2.134 – 4.312)
x_2 (mM)	0.246 ± 0.012** (0.221 – 0.270)	0.246 ± 0.012** (0.221 – 0.270)	0.246 ± 0.012** (0.221 – 0.270)	0.246 ± 0.012** (0.221 – 0.270)
β_2 (%/mM)	-2.731 ± 0.232** (-3.205 – 2.257)	-2.731 ± 0.232** (-3.205 – 2.257)	-2.731 ± 0.232** (-3.205 – 2.257)	-2.731 ± 0.232** (-3.205 – 2.257)
ED_{-10L} (mM)	0.026 ± 0.002** (0.022 – 0.030)	-	-	-
LDS (mM)	-	0.219 ± 0.005** (0.210 – 0.230)	-	-
ED_{50} (mM)	-	-	0.343 ± 0.010 (0.323 – 0.362)	-
M (mM)	-	-	-	0.086 ± 0.004** (0.078 – 0.094)
ymax (%)				150.758
R^2 (R^2 adj)	0.995 (0.994)	0.995 (0.994)	0.995 (0.994)	0.995 (0.994)
c= 0, *d* = 100				
c (%) fixed	0.000	0.000	0.000	0.000
d (%) fixed	100.000	100.000	100.000	100.000
x_1 (mM)	0.052 ± 0.007** (0.038 – 0.066)	0.052 ± 0.007** (0.038 – 0.066)	0.052 ± 0.007** (0.038 – 0.066)	0.052 ± 0.007** (0.038 – 0.066)
β_1 (%/mM)	2.881 ± 0.514** (1.832 – 3.931)	2.881 ± 0.514** (1.832 – 3.931)	2.881 ± 0.514** (1.832 – 3.931)	2.881 ± 0.514** (1.832 – 3.931)
x_2 (mM)	0.230 ± 0.022** (0.185 – 0.274)	0.230 ± 0.022** (0.185 – 0.274)	0.230 ± 0.022** (0.185 – 0.274)	0.230 ± 0.022** (0.185 – 0.274)
β_2 (%/mM)	-2.199 ± 0.158** (-2.521 – -1.878)	-2.199 ± 0.158** (-2.521 – -1.878)	-2.199 ± 0.158** (-2.521 – -1.878)	-2.199 ± 0.158** (-2.521 – -1.878)
ED_{-10L} (mM)	0.026 ± 0.002** (0.022 – 0.030)	-	-	-
LDS (mM)	-	0.216 ± 0.005** (0.205 – 0.227)	-	-
ED_{50} (mM)	-	-	0.365 ± 0.008** (0.348 – 0.381)	-
M (U/mL)	-	-	-	0.086 ± 0.004** (0.077 – 0.095)
ymax (%)				153.053
R^2 (R^2 adj)	0.993 (0.992)	0.993 (0.992)	0.993 (0.992)	0.993 (0.992)

[a]Data are given as mean ± standard error with 95% confidence interval in parentheses. **P < 0.0001for all estimated parameters. *P < 0.01for the estimated parameters.

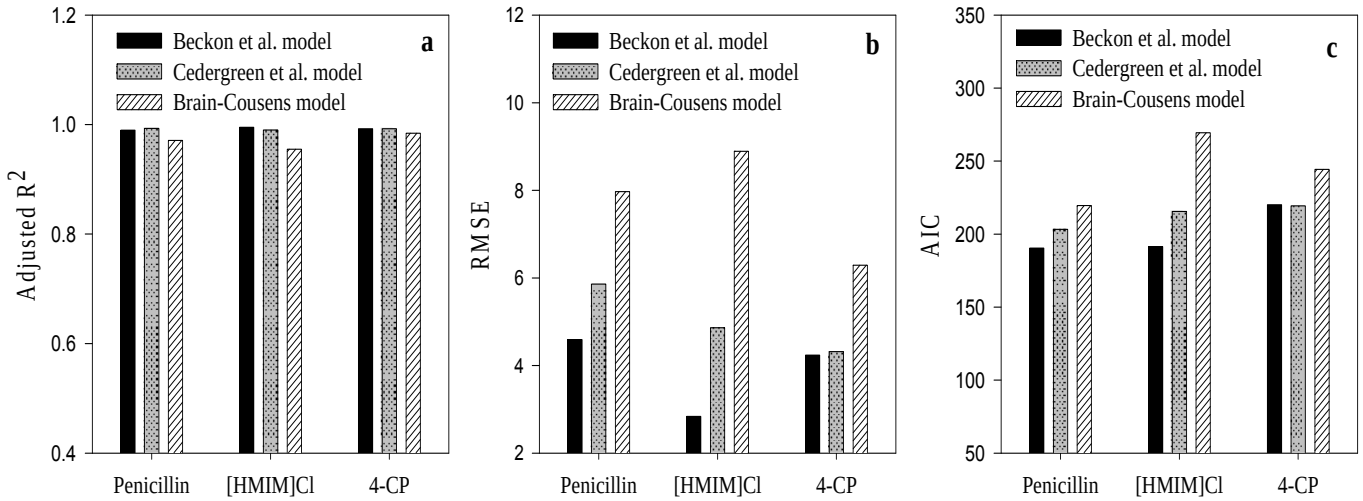

Figure 4. Goodness-of-fit statistics (a: Adjusted R^2, b: RMSE and c: AIC) for Beckon et al. (2008), Cedergreen et al. (2005) and Brain-Cousens models describing the three data sets (Penicillin, [HMIM]Cl and 4-Chlorophenol [4-CP]).

Table 6. Comparison of effective doses derived from the hormesis models for the three data sets

Effective doses[a]	Model		
	Brain-Cousens	Cedergreen-Ritz-Streibig	Beckon et al. (Bilogistic)
Penicillin (U/mL)			
ED_{50}	0.032 ± 0.001* (0.030 – 0.034)	0.032 ± 0.001* (0.030 – 0.033)	0.032 ± 0.001* (0.031 – 0.333)
LDS	0.023 ± 0.001* (0.022 – 0.024)	0.022 ± 0.0004* (0.022– 0.023)	0.023 ± 0.0004* (0.022 – 0.024)
ED_{-10R}	0.022 ± 0.001* (0.020 – 0.023)	0.017 ± 0.0004* (0.020 – 0.022)	0.021 ± 0.0004* (0.0214 – 0.0223)
ED_{-10L}	0.0015 ± 9.818 E-5* (0.0013 – 0.0017)	0.0028 ± 0.0003** (0.0022 – 0.0034)	0.0035 ± 0.0003** (0.0029 – 0.0040)
M	0.0119± 0.0005* (0.0108 – 0.0129)	0.0115 ± 0.0003* (0.0108 – 0.0122)	0.0101 ± 0.0005* (0.0090 – 0.0112)
ymax (%)	159.647	165.182	161.038
[HMIM]Cl (M)			
ED_{50}	0.089 ± 0.004* (0.080 – 0.097)	0.088 ± 0.002* (0.084– 0.091)	0.088 ± 0.001* (0.086 – 0.090)
LDS	0.055 ± 0.002* (0.051– 0.059)	0.060 ± 0.001** (0.058 – 0.062)	0.062 ± 0.001** (0.060 – 0.063)
ED_{-10R}	0.051 ± 0.002* (0.047 – 0.054)	0.056 ± 0.001** (0.053 – 0.058)	0.057 ± 0.001** (0.055– 0.058)
ED_{-10L}	0.0026 ± 0.0002* (0.0021 – 0.0031)	0.0009 ± 0.0002** (0.0006 – 0.0012)	0.0014 ± 0.0001** 0.0011– 0.0016)
M	0.024 ± 0.001* (0.021 – 0.026)	0.026 ± 0.001* (0.024 – 0.027)	0.022 ± 0.001* (0.020 – 0.024)
ymax (%)	158.161	154.655	148.944
4-CP (mM)			
ED_{50}	0.358 ± 0.010* (0.337 – 0.379)	0.360 ± 0.008* (0.344 – 0.375	0.365 ± 0.008* (0.348 – 0.381)
LDS	0.223 ± 0.006* (0.210 – 0.236)	0.214 ± 0.005* (0.204 – 0.223)	0.216 ± 0.005* (0.205 – 0.227)
ED_{-10R}	0.204 ± 0.006* (0.190 – 0.217)	0.195 ± 0.005* (0.185 – 0.204)	0.026 ± 0.002** (0.022 – 0.030)
ED_{-10L}	0.014 ± 0.001* (0.012 – 0.016)	0.024 ± 0.002** (0.021 – 0.028)	0.026 ± 0.002** (0.022 – 0.030)
M	0.102 ± 0.004* (0.093 – 0.112)	0.093 ± 0.003* (0.088 – 0.099)	0.086 ± 0.004* (0.077 – 0.095)
ymax (%)	146.894	153.317	153.053

[a]Data are given as mean ± standard error with 95% confidence interval in parentheses. c= 0, d = 100. Within rows, for each parameter derived from different models and same hormesis data, values with same number of asterisks are not significantly different from each other ($p > 0.05$).

parameters is therefore a prerequisite to successful curve fitting of a nonlinear model with many parameters. The ease of this selection depends on the interpretability of the parameters. Practically-interpretable parameters often lead to better initial parameter estimate and consequently simplify the model fitting process (Mcmeekin et al., 1999). This is because the initial parameter value can easily be deduced from the *x-y* plot of the observed data. Some parameters of the bilogistic model (such as d, c, x_1, x_2, ED_{-10}, ED_{50}. *LDS* and *M*) are interpretable and can be easily deduced from *x-y* plot of the observed data. Other parameters cannot be easily deduced from the observed data. For instance, *Max* is a theoretical maximum response to be reached by rising curve in the absence of descending curve or vice versa.

The interpretation of *Max* is not in agreement with its fitted value. Other parameters that cannot easily be deduced are the slope parameters β_1 and β_2. However, the fact that β_1 must have a positive value while β_2 must have a negative value would be helpful. Selecting good initial estimates for such non interpretable parameter can be time consuming and require some kind of experience. However, the process of selecting good initial estimates to ensure convergence is simplified with TableCurve 2D. By supplying the values of the interpretable parameters and making smart guess of the values of non-interpretable parameters to make the regression line somehow close to observed data, the initial estimates of all parameters can be updated automatically to optimal values in TableCurve 2D. In doing this, care must be taken to ensure that unrealistic values are not produced especially in cases (like ED_{-10}) where two values are possible. In Table Curve 2D, and possibly other statistical softwares, application of constraint on ED_{-10} may not be critical. The initial parameter estimate for any particular ED_{-10} (ED_{-10L} or ED_{-10R}) could be optimized in TableCurve 2D by selecting value around the required ED_{-10}. Since ED_{-10} is an interpretable parameter, this approach of using graphically-deduced initial estimates can simply be applied to estimate ED_{-10L} or ED_{-10R} without applying constraint.

Another practical challenge observed in fitting the bilogistic model is the poor estimation properties of the upper (d) and lower (c) asymptotes. When allowed to be estimated iteratively, unrealistic negative values of the lower asymptote were produced in the *Staphylococcus* sp. and luciferase data sets. In these data sets, there was no obvious saturation of effect at infinite doses. Similarly,

estimation of upper asymptote (*d*) could result to values with wide standard error and 95% confidence limit. As pointed out by Schabenberger et al. (1999), it is important to consider whether estimation of lower (*c*) and upper (*d*) asymptotes is necessary. In our data, theoretical considerations suggested that the lower and upper asymptotes should be 0 and 100%, respectively. The statistical properties of other model parameters improved when *c* and *d* were fixed as 0 and 100%, respectively. The reparameterization of the bilogistic models is the substitution of *Max* with a function containing interpretable parameters. Generally, these extensions did not affect estimation of other parameters and goodness-of-fit especially when the value of c and d were fixed. However, minor variations which are not statistically significant may occur. Thus, the values of ED_{-10}, *LDS*, ED_{50} and *M* were estimated with good statistical properties. In addition, the value of y_{max} was slightly affected when *c* and *d* were fixed.

The reparameterized models were successfully applied to estimate effective doses and their confidence intervals. Although reparameterization of models was discouraged by Cedergreen et al. (2005) and recommended the use of bisection and delta methods implemented in some statistical software, delta method could only allow the estimation of ED_K doses with statistical properties and to extract *M* without statistical properties. In addition, the mathematical operation is not implementable in some statistical software. The reparameterized models can easily be coded into any curve fitting statistical software. Hence, the approach as recommended by Cedergreen et al. (2005) may not be easier than reparameterization for some users (Nweke and Ogbonna, 2017). Furthermore, the limitations of the delta method with respect to statistical properties of *M* underline the importance of reparameterization as an alternative approach for exploration of hormesis quantities in hormetic dose-response relationships. The competitiveness of this approach remains a pending question that is worth exploring (Belz and Piepho, 2012).

Conclusion

This study described a general approach to estimate the effective doses at hormetic and toxic dose ranges in inverted U-shaped dose-response relationships by reparameterization of a bilogistic model. The extended models were successfully applied to test for significance of hormesis and estimate effective doses and their confidence limits by non-linear curve fitting. Therefore, the suggested reparameterizations would result in accurate determination of the effective doses, their standard errors and confidence limits in dose (concentration)-response relationships that could be best described by the bilogistic model. The use of the bilogistic model where it is most suitable will help to remove errors that may arise from the use of other hormesis models that do not adequately represent the data. In addition, the models will be applicable in the study of variability of inverted U-shaped dose-response relationships in many disciplines. These models could potentially help to refine regulatory guidelines for protection of human, animal, plant and microbial populations which would have bearing upon the management of environmental health.

CONFLICT OF INTERESTS

The authors have not declared any conflict of interests.

REFERENCES

Beckon WN, Parkins C, Maximovich A, Beckon AV (2008). A general approach to modeling biphasic relationships. Environmental Science & Technology 42(4):1308-1314.

Belz RG, Cedergreen N, Duke SO (2011). Hericide hormesis – can it be useful in crop production? Weed Research 51(4):321-332.

Belz RG, Cedergreen N (2010). Parthenin hormesis in plants depends on growth conditions. Environmental and Experimental Botany 69(3):293-301.

Belz RG, Leberle C (2012). Low dose responses of different glyphosate formulations on plants. Proceedings of 25th German Conference on Weed Biology and Weed Control, March 13-15, Braunschweig, Germany.

Belz RG, Piepho HP (2012). Modeling effective dosages in hormetic dose-response studies. Plos One 7(3):1-10.

Belz RG, Piepho HP (2015). Statistical modeling of the hormetic dose zone and the toxic potency completes the quantitative description of hormetic dose responses. Environmental Toxicology and Chemistry 34(5):1169-1177.

Brain P, Cousens R (1989). An equation to describe dose responses where there is stimulation of growth at low doses. Weed Research 29(2):93-96.

Cedergreen N, Felby C, Porter JR, Streibig JC (2009). Chemical stress can increase crop yield. Field Crops Research 114(1):54-57.

Cedergreen N, Olesen F (2010). Can glyphosate stimulate photosynthesis? Pesticide Biochemistry and Physiology 96(3):140-148.

Cedergreen N, Ritz C, Streibig JC (2005). Improved empirical model describing hormesis. Environmental Toxicology and Chemistry 24(12): 3166-3172.

Cedergreen N, Streibig JC, Kudsk P, Stephen O, Duke SO, Mathiassen SK (2007). The occurrence of hormesis in plants and algae. Dose-Response 5(2):150-162.

Li Y, Zhang B, He X, Cheng W-H, Xu W, Luo Y, Liang R, Lao H, Huang K (2014). Analysis of individual and combined effects of Ochratoxin A and zearalenone on HepG2 and KK-1 cells with mathematical models. Toxins 6(4):1177-1192.

Migliore L, Godeas F, De Filippis SP, Mantovi, P, Bonazzi G, Barchi D, Testa C, Rubattu N, Rambilla G (2010). Hormetic effect(s) of tetracyclines as environmental contaminant on *Zea mays*. Environmental Pollution 158(1):129-134.

Mulkiewicz E, Jastorfi B, Skladanowski AC, Kleszczyński K, Stepnowski P (2007). Evaluation of the acute toxicity of perfluorinated carboxylic acids using eukaryotic cell lines, bacteria and enzymatic assays. Environmental Toxicology and Pharmacology 23(3):279-285.

Murado MA, Vázquez JA (2010). Basic toxicodynamic features of some antimicrobial agents on microbial growth: a dynamic mathematical model and its implications on hormesis. BMC Microbiology 10(1):1-14

Mcmeekin TA, Olley JN, Ross T, Ratkowskey DA (1999). Predictive Microbiology, Theory and Applications. John Wiley. New York p. 68.

Nweke CO, Ahumibe NC, Orji JC (2014). Toxicity of binary mixtures of formulated glyphosate and phenols to *Rhizobium* species dehydrogenase activity. Journal of Microbiology Research 4(4):161-169.

Nweke CO, Ike CC, Ibegbulem CO (2016). Toxicity of quaternary mixtures of phenolic compounds and formulated glyphosate to microbial community of river water. Ecotoxicology and Environmental Contamination 11(1):63-71.

Nweke CO, Orji JC, Ahumibe NC (2015). Prediction of phenolic compound and formulated glyphosate toxicity in binary mixtures using *Rhizobium* species dehydrogenase activity. Advances in Life Sciences 5(2):27-38.

Nweke CO, Ogbonna CJ (2017). Statistical models for biphasic dose-response relationship (hormesis) in toxicological studies. Ecotoxicology and Environmental Contamination 12(1):39-55.

Shen K, Shen C, Lu Y, Tang X, Zhang C, Chen X, Shi J, Lin Q, Chen Y (2009). Hormesis response of marine and freshwater luminescent bacteria to metal exposure. Biological Research 42(2):183-187.

Schabenberger O, Tharp BE, Kells JJ, Penner D (1999). Statistical test for hormesis and effective dosages in herbicide dose–response. Agronomy Journal 91(4):713-721.

Van Ewijk PH, Hoekstra JA (1993). Calculation of the EC50 and its confidence interval when subtoxic stimulus is present. Ecotoxicology and Environmental Safety 25(1):25-32.

Wang LJ, Liu SS, Yuan J, Liu HL (2011). Remarkable hormesis induced by 1-ethyl-3-methyl imidazolium tetrafluoroborate on *Vibrio qinghaiensis* sp.-Q67. Chemosphere 84(10):1440-1445.

Wang HW, Wang JQ, Zheng BQ, Li SL, Zhang SL, Li FD, Zheng N (2014). Cytotoxicity induced by ochratoxin A, zearalenone, and a-zearalenol: Effects of individual and combined treatment. Food and Chemical Toxicology 71:217-224.

Zelaya IA, Owen MDK (2005). Differential response of *Amaranthus tuberculatus* (Moq ex DC) JD Sauer to glyphosate. Pest Management Science 61(10):936-950.

Zhu XW, Liu SS, Qin LT, Chen F, Liu HL (2013). Modeling non-monotonic dose response relationships: Model evaluation and hormetic quantities exploration. Ecotoxicology and Environmental Safety 89:130-136.

Zou X, Lin Z, Deng Z, Yin D (2013). Novel approach to predicting hormetic effects of antibiotic mixtures on *Vibrio fischeri*. Chemosphere 90(7):2070-2076.

Related Journals: